UNIVERSITY OF TROMSØ UIT

FACULTY OF SCIENCE
DEPARTMENT OF PHYSICS AND TECHNOLOGY

Design and Evaluation of a Medical Microwave Radiometer for Observing Temperature Gradients Subcutaneously in the Human Body

Øystein Klemetsen

A dissertation for the degree of Philosophiae Doctor
November 2011

To my family

When you can measure what you are speaking about, and express it in numbers, you know something about it. But when you cannot measure it, when you cannot express it in numbers, your knowledge is of a meagre kind. It may be the beginning of knowledge, but you have scarcely in your thoughts advanced to the stage of science.

— Lord Kelvin (1824-1907)

Abstract

The topic covered in this thesis is medical temperature measurement of subcutaneous parts of human tissue with use of microwave radiometry. Radiometry is a completely non-invasive, non-toxic and relatively inexpensive sensing modality. The radiometric technique is based on the measurement of electromagnetic noise power emitted by lossy materials. The method has explicit low investment costs and low technological complexity, but relatively low spatial resolution. Still the method can be useful for some dedicated medical applications.

Fundamental radiometric theory and dielectrical properties of biological tissues are derived. The process to realize a miniaturized radiometer is going from active antenna configuration to a complete miniaturized radiometer and finally to a modular radiometer, that is used *in-vivo* on humans.

Different radiometers were designed, simulated, built and tested on realistic human phantoms. *In vivo* experiments were also conducted to verify the prototype radiometer and to test the ability to be used in tailored medical diagnostics. The primary application covered is temperature gradient measurement during microwave hyperthermia and in pediatric vesicouretaral reflux (VUR) detection. Hyperthermia is a therapeutic technique in which cancerous tissue is heated to 40-45°C, inducing vascular and cellular changes that improve the therapeutic effectiveness when used in conjunction with chemotherapy or radiation therapy. VUR is abnormal flow of urine from the bladder back to the upper urinary tract. Another application where this radiometer can be of great interest is in breast cancer diagnostic. Breast cancer is a type of cancer that forms in tissues of the breast; usually in the ducts and lobules and can occur in both men and woman.

We present results from radiometric measurement on human phantoms during a hyperthermia heating sequence. Experimental evidence shows that radiometry can be used for temperature quality assurance of the heated volume in depth.

In VUR detection, the first step is to heat the bladder prior to detection of the reflux. We present results from measurements *in-vivo* with a water filled balloon in the human mouth, that mimics pediatric bladder heating. Results show that the radiometer can be used as the first step in the novel VUR detection.

Radiometry antennas are one of the most critical components in a radiometer system. An elliptical printed circuit board antenna is designed and matched to the human body. Further, an antenna with suction, with use of negative pressure to mount the antenna onto the human body for improved radiometric performance, was also proposed and built. The simple and elegant solution for the coupling of the antenna with use of negative pressure, documents improved performance in estimating the true temperature as well as exhibiting smaller fluctuation in the radiometric signal.

Acknowledgements

My most sincere and deep gratitude goes to my supervisor Professor Svein Jacobsen for the opportunity to work with such an exciting field. Your insight, advice, technical expertise and encouragement helped me many times in the work of this thesis. Svein, I appreciate that I had the opportunity to spend my foreign stay at one of your collaborators in the United States. I also appreciate all the hours we spent together during the various experiments we conducted together. Not least, I thank you for all the discussions we had, both professional and non-professional. I must also thank you for all suggestions and improvements in the writing of this thesis.

I would also like to thank my co-supervisor Associate Professor Yngve Birkelund for all academic support and especially your rush to get me to start writing conference papers during our common stay in the U.S.

I thank the University of Tromsø for support and the opportunity to also work in Harstad, where my family and I are staying.

Professor Paul Stauffer, I owe you a big thanks. You invited me to spend a great year at Duke University, USA. I am very grateful for having had this opportunity, and not least to be a part of the research group working with vesicoureteral reflux (VUR) detection. I thank the others on the research group: Assistant Professor Paolo Maccarini, Dr. Kavitha Arunachalam, Valeria De Luca, Sara Salahi, Dr. Cory Wyatt and Associate Professor Yngve Birkelund, for all the support, discussions, and especially all the social events we shared.

I would also like to thank ThermImage, Salt Lake City, Utah, USA with Professor Brent Snow, at University of Utah in the lead for the opportunity to investigate the VUR issue. Not least, I am very grateful that I was invited by ThermImage in an incredibly exciting animal experiment in Salt Lake City, where I learned a lot.

Senior Engineer Karl Magnus Fossan, I thank you for all the discussions we had. Most of all, I appreciate your very friendly manner that encouraged me to continue as a PhD student, when I most wanted to quit in the first years.

Also, I thank my first office roommate Heidi Hindberg and second roommate Wojciech Miloch for all the company. Without you, there have been very lonely days in the office.

My family supported me in my efforts since I first became a student and to this day, thanks mom, dad and mother in law. Not least, I thank my wife Inger for all the encouragement, support and patience when I commuted to Tromsø. Without your help this thesis has never been realized. I am forever grateful to you. I would also like to thank my son Eskil and daughter Ingrid for the patience they have shown when dad was away on lodgings. One of the things that I will remember best from this period is our fantastic trip to the United States, not to mention the Grand Canyon.

Øystein — Harstad, November 15, 2011

Contents

List of Tables

List of Figures

Chapter 1

Introduction

Medical imaging methods have a major impact on how to improve the effectiveness of modern health care. There is obviously a need to acquire 2-D images of, or volumetric scans within, the human body in medical diagnostics. This technology is surely among the most important tools in western medicine. A range of medical imaging modalities are in use in today's public health service [Sprawls, 1987, Hendee and Ritenour, 2002, Iniewski, 2009]. Very few of the methods provide both low investments and running costs. Some methods exhibit relatively low investment costs, but high running-costs. Others again, and often more sophisticated methods, are associated with both high investment and running costs. The availability of the latter category for large patient groups has become a political question.

Different diseases require imaging techniques tailored to the particular disease or anatomical survey, while other more flexible systems can be used in many different cases and illnesses [Gotthardt et al., 2010]. All imaging techniques have their advantages and disadvantages depending on what set of criteria (performance indices) that is used. Nevertheless, ever more sophisticated methods have been developed in recent decades due to increased capacity of data acquisition and effectiveness of image processing. Established methods are further developed with new technology that allows easier handling, storage and interpretation of medical images [Egan and Liu, 1995]. As an example, X-ray images on analog film are rare nowadays and thus almost completely replaced by digitized imagery. Research results on advanced imaging processing algorithms using pattern recognition and image segmentation are continuously implemented in updated versions of medical equipment [Egan and Liu, 1995].

The increase in number of examinations performed in modern healthcare, combined with continually novel imaging modalities becoming available, have resulted in that significantly more medical sessions are taking place. This has made the need for systems able to acquire, distribute and store vast amounts of medical data [Pavlopoulos and Delopoulos, 1999]. Improved quality in medical images is essential to improve diagnostic effectiveness in a shorter examination time. However, the growing number unnecessary medical image scans performed every year contributes to excessive medical running costs [AHIP, 2008]. Hence, there seems to be a need for non-invasive imaging

tools that can be used in clinics, by family doctors and in modern telemedicine to reduce patient travelling which again will reduce health care costs. Many studies point out the need for telemedicine because of less human resources required in the treatment and follow-up phases [Norris, 2002, Obstfelder et al., 2007, Broens et al., 2007]. Further, cheap, readily available, small sized and easy-to-use medical imaging instrumentation is one way to reduce the above mentioned resource factors. A non-invasive medical radiometer is one such device that has the potential to be used by many health care providers. With the above aspects in mind, we will look at different methods and principles to produce medical images.

1.1 Medical Imaging Methods

There are a multitude of medical imaging modalities in modern medicine, ranging from the well known and widely used ionized X-ray method to passive modalities as e.g. infrared (IR) or microwave thermography. All medical imaging methods have its pros and cons. But, the purpose of generating a medical image may be to transform information that contributes to detection of a disease or injury; describing its nature and extent; diagnosis of the subject causing the disease or injury; guidance of treatment; or monitoring the treatment and its consequences [Hendee and Ritenour, 2002]. The extent to which it is possible to perform the above factors highly depends on the image quality. The clarity of an image is how informative the image displays the information in an image, and is influenced by fundamentals factors such as: blur or unsharpness, distortion and artifacts, as well as contrast and noise [Hendee and Ritenour, 2002, Sprawls, 1987].

The most detrimental effect of image blur is the reduction of visibility of details in the image. Image blurring due to patient motion is a well known problem in medical modalities. This unwanted effect typically occurs if the patient moves during image acquisition, but also involuntary and uncontrollable motions of internal organs can be a contributing factor. Blur in medical images induced by patient motion is one of the most frequently cited reasons for image rejection in radiographic diagnostic imaging [Luo et al., 2008]. However, general blur and artifacts are a challenge in all medical imaging modalities. Artifacts are structures in an image that do not represent a body object. Examples include streaks caused by moving structures of high density in computed tomography, artifacts produced by nonuniformities in the magnetic field introduced by metallic structures in MRI and reverberation artifacts in ultrasound [Hendee and Ritenour, 2002]. Image distortion is also caused by unequal magnification of various structures in the image. An internal object should be viewed in the right position, with correct size and shape without too much distortion introduced [Sprawls, 1987]. Object contrast is the contrast between two adjacent areas in a medical image and plays an important role in the ability to perceive image details. In medical imaging, the contrast of an image is a product of complex interactions among the anatomic and physiologic attributes of the region of tissues [Hendee and Ritenour, 2002]. To provide a signal difference from the surrounding tissues, contrast media can be used.

Noise is a problem to various extent in all electronics. Image noise is most significant on low-contrast objects that are close to the visibility threshold and may affect the boundary between the visible and invisible object.

1.1.1 Ionization X-ray

X-ray imaging, and its 3-D extension named computed tomography (CT), use high energy photons in an incoherent beam to penetrate the human body. The absorption, transmission and scatter of the photons form the image; nowadays in a digital detector array. Mammography uses low-dose X-ray equipment to obtain images of the breast to assist in the diagnosis of breast cancer and other breast diseases. Fluoroscopy is an imaging method that uses X-rays and a monitor to produce real time images of the body. Typically, fluoroscopy is used to image the hepato-biliary system, digestive tract and genitourinary system in clinical radiology departments. CT systems use several beamshots from different angles to form an image, and thus expose the human body to more ionizing radiation than the conventional X-ray. CT is one of the largest contributors to radiation doses in medical populations, and the principal concern regarding radiation exposure is that the modality may induce malignancies. Nevertheless, the effective dose for a chest CT is approximately 100 to 1000 times larger than that for a corresponding chest X-ray examination [Semelka et al., 2007].

A CT image is reconstructed mathematically from the measured data [Kalender, 2006]. The patient lies on a couch that moves through the imaging gantry with X-ray tube and a detector array.

1.1.2 Nuclear Imaging

Nuclear diagnostic can be used in localization of malignant tissue, to see different types of flow, looking at dilution and to reveal biochemical and metabolic properties [Hendee and Ritenour, 2002]. The patient is injected with a radioactive drug and radioactivity decays are emitting gamma rays. A gamma camera, or scintillation camera, is a device that takes a picture of high-energetic photons from a gamma-emitting radioactive source, similar to how a conventional camera takes a picture of an illuminated object.

Positron emission tomography (PET) is a modality within radionuclide tomographic imaging, and is based on an unique characteristic of the radiation associated with positrons. Positrons are particles of anti-matter and the mass is like that of the electron. When the positron interacts with an electron, there is an annihilation and the converted energy is a pair of photons that leaves the site in precisely opposite directions. This phenomenon makes tomographic imaging possible [Sprawls, 1987]. The emission of positrons comes from radioactive pharmaceuticals.

Single-photon emission computed tomography (SPECT) is the technique for tomographic images with conventional radionuclides that emits only one photon per nuclear transition and uses a gamma camera as the imaging device. The imaging device rotates

around the human body and collects data in a projection-based manner. PET has better spatial and temporal resolution and better sensitivity compared to SPECT. PET/CT is a novel and evolutionary imaging modality that combine both CT and PET in the same scanner [Townsend et al., 2004].

1.1.3 Non Ionization Radiation

Magnetic resonance imaging (MRI) is a non-ionizing modality and is regarded as safer than many other techniques. MRI provides excellent soft tissue contrast and is useful for oncological, neurological, cardiovascular and musculoskeletal imaging [Iniewski, 2009]. MRI detects signals predominantly from hydrogen nuclei in the tissues and has the ability to create flowing blood images without use of contrast media [Sprawls, 1987]. The patient is placed in a strong magnetic field and a pulse train of radio waves is transmitted from an antenna that is a typical coil-antenna positioned around the patient. The principle of MRI is to display the intensity of the emitted radio frequency from nuclear spin in the tissue after a magnetization of the tissue. MRI is not as sensitive as PET or SPECT, or as fast as CT, but MRI can generate a great variety of contrast images for a wide range of applications. The anatomical details provided by MRI and CT give a better structural description of organs by resolving capabilities that are significantly higher than that provided by PET and SPECT. CT and MRI provide a resolution in the sub millimeter range and also produce better tissue contrast, especially in the presence of contrast media [Stout and Zaidi, 2008].

Ultrasound

Ultrasound imaging forms images of biological tissue by transmitting focused beams of sound waves into the body and receive echoes from structural interfaces within the body [Iniewski, 2009]. During the propagation of an ultrasonic wave, the particles of the matter vibrate over very short distances in a direction parallel to the longitudinal wave. It is this vibration process, during which momentum is transferred among particles, that causes the wave to move through the matter [Sprawls, 1987]. The velocity of the pulses changes as it passes from one material to another, but this variation is relatively small, except for some material as e.g. bone. In low-density media such as air and gases, molecules may move over relatively large distances before they influence neighboring molecules. In these media, the velocity of an ultrasound wave is low. In solids, molecules are constrained in their motion, and the velocity of ultrasound is high. In liquids the velocity is in between gases and solids. Further, in biological tissues, the velocity is roughly the same as in liquids [Hendee and Ritenour, 2002]. The time interval between the transmitted and the received pulse is related to the distance to the reflected interface and is used to form an image. The resolution can be improved by using sound waves from several angles. Ultrasound is used clinically to e.g. discover whether a lesion detected from a mammographic examination is a liquid cyst or a solid tumor. Frequencies

of 1 MHz and above are required to furnish ultrasound wavelengths suitable for diagnostic imaging [Hendee and Ritenour, 2002]. Nearly all pregnant women in western countries, experience to see their developing fetus with this technology.

Due to the small area of the transducer and reduction in power and size of electronics, the ultrasound has been under a miniaturization process and that without loss of performance [Iniewski, 2009]. Today, ultrasound can be used with a smartphone and a mobile application, and is cleared by US Food and Drug Administration (FDA) [Mob, 2011, Smith et al., 2010].

Furthermore, a large improvement in lateral resolution and signal-to-clutter ratio can be obtained for the higher harmonics of the ultrasound because the nonlinear behavior of the medium is exploited in medical applications [Averkiou et al., 1997, Christopher, 1998, Haider and Chiao, 1999, Varray et al., 2011]. Second harmonic ultrasound is typically obtained with a transmitter on one frequency, then the receiver operate at both the first and second harmonic of the transmitted frequency [Schrope and Newhouse, 1993]. This technique is used in e.g. brain tissue perfusion and blood perfusion measurements [Schrope and Newhouse, 1993, Harrer et al., 2003]. Moreover, ultrasound technology is also used in a hybrid system where the tissue is heated by microwave energy and the ultrasounds detect the pressure waves generated by tissue expansion [Zhurbenko, 2011].

Ultra Wide Band Radar

Applying ultra wide band (UWB) technology in medical applications is an emerging research trend in recent years [Hagness et al., 1998, Fear et al., 2002b, Staderini, 2002, Fear et al., 2002a, Fear et al., 2002c, Xie et al., 2006, Jacobsen and Birkelund, 2010]. UWB is an active detection modality and uses electrical properties of e.g. breast tissues to obtain a contrast between malignant and healthy breast tissues. UWB microwave radar views a target using scattered microwaves. The principle involves illuminating the tissue with microwave energy and then forming the image of the tissue with the transmitted energy reflected or through the tissue [Xie et al., 2006, Fear et al., 2002a], much like tomography image reconstruction and ultra wideband confocal microwave imaging (CMI). UWB CMI uses microwave pulses that are transmitted from antennas at different positions on the tissue surface. The backscattered energy response from the tissue is then recorded and calculated using simple and effective signal processing algorithms to form an image. Other applications for UWB can be patient motion monitoring in emergency room, at home and in pediatric clinics [Ossberger et al., 2004, Zito et al., 2007, Staderini, 2002].

1.1.4 Natural Thermal Radiation

Heat can transfer by three main modes: i) The first, conduction, which requires contact between the objects, ii) convection, where the flow of hot mass transfers thermal energy and iii) radiation. Heat transfer by radiations is of great value in medicine [Diakides

and Bronzino, 2008]. Natural thermal radiation is the electro-magnetic (EM) radiation from all objects that have a temperature above absolute zero kelvin.

Infrared Thermography

Infrared (IR) thermography can be used to seek tumors by its infrared signature. The most basic design consists of a lens to focus the infrared energy onto a detector. The passive infrared thermograph has excellent spatial resolution but is not able to see in depth of a lossy medium. The infrared imaging approach can be used e.g. in breast cancer detection [Head and Elliott, 2002, Diakides and Bronzino, 2008], imaging varicose and subcutaneous veins [Zharov et al., 2004], vein pattern biometric [Wang and Leedham, 2006] and determining inflammatory [Chang et al., 2008].

Microwave Thermography

In clinical medicine, microwave radiometry is used to obtain information about internal body temperature patterns by measurement of the natural thermal radiation from the

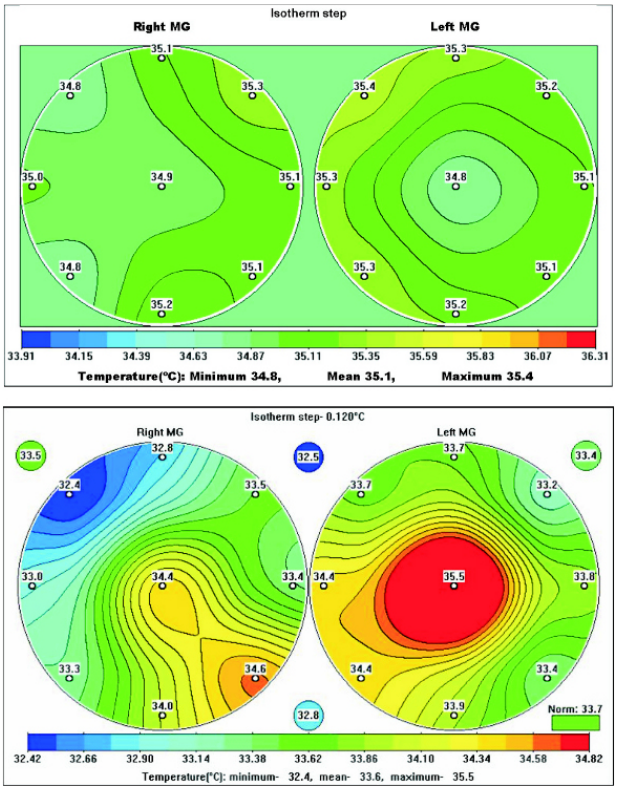

Figure 1.1: Microwave radiometry image of human breast [Vesnin, 2011]. The top two images are of healthy breasts. Bottom left is a healthy breast and bottom right is a breast with cancer.

tissues of the human body. The technique is noninvasive, inherently completely safe, and can be used to form an image with low resolution. An example is given in figure 1.1 where 9 probe responses from a breast are used to form the image.

1.1.5 Summary of Imaging Modalities

Since costs are defined as the value of the resources used, the cost each medical imaging modality represents can be divided into fixed costs and variable costs [Ohinmaa et al., 2001]. Fixed costs or investment cost can be; investment in machinery, education of personnel and support services, machinery room, software and annual service costs of the equipment. Variable costs (or running costs) of delivering medical images are more diffuse, due to the many available modalities. For more information about this general aspect, I refer to the work of Bryan *et al.* [Bryan et al., 2000].

Hardware complexity and image resolution of each medical imaging modality are important factors, and a good overview can be found in several books [Iniewski, 2009, Bushberg et al., 2002, Hendee and Ritenour, 2002, Sprawls, 1987]. Presently, to compare the costs of each medical imaging modality, I have only taken investment costs into account.

To compare the above mentioned medical imaging methods, investment cost, hardware complexity and image resolution of the different methods, are summarized in table 1.1.

1.2 Motivation to use Microwave Radiometry in Medicine

Microwave radiometry has explicit low investment costs and low technological complexity, but however low spatial resolution compared to the other modalities as seen in

Table 1.1: Comparison of imaging methods in medicine.

Modality	Investment cost	Hardware complexity	Resolution
X-ray	Moderate	Moderate	High
CT	High	High	High
PET	High	High	High
SPECT	High	High	High
Gamma camera	Moderate	Moderate/High	Moderate
MRI	High	High	High
Ultrasound	Moderate	Moderate	Moderate
UWB	Low/Moderate	Low	Moderate
IR	Moderate	Moderate/High	High
Microwave radiometry	Low	Low	Low

table 1.1. Other advantages of this method are that it can see at depth of the human body and instrumentation and applicator can be made practically small. Thus, it is especially useful for some dedicated medical applications, to be discussed below:

- Breast cancer is a type of cancer that forms in tissues of the breast; usually in the ducts and lobules and can occur in both men and woman. Breast cancer is expected to account for 26% of all new cancer cases among women in the year 2008 in United States [Jemal et al., 2008]. The gold standard for early detection of breast cancer has since the 1960s been mammography [Kennedy et al., 2009]. The risk of mammography is radiation exposure [Sprawls, 1987, Guyton and Hall, 2000] as well as rupture risk of the encapsulation of the cancer tumor when the breast is compressed [Kennedy et al., 2009]. Microwave radiometry was proposed in the seventies as a diagnostic method to detect breast cancer using a non-invasive procedure that avoids these problems [Enander and Larson, 1974, Barrett and Meyers, 1975].

- Vesicoureteral reflux (VUR) is abnormal flow of urine from the bladder back to the upper urinary tract. The urinary tract includes kidneys, ureters, bladder, and urethra. Blood flows through the kidneys, and the kidneys filter out wastes and produce urine. The urine travels down from the kidney via two narrow tubes called the ureters. The urine is then stored in the bladder. Normally, when the bladder empties, urine flows out of the body through the urethra at the bottom of the bladder. In case of VUR, urine flows back into one or both ureters and, in some cases, to one or both kidneys. VUR is most common in infants and young children, but older children can also be affected. VUR is internationally classified in grade I to V, where grade I is reflux into non-dilated ureter and grade V is gross dilatation of the ureter, pelvis and calyces; ureteral tortuosity; loss of papillary impressions [Snow and Taylor, 2010].

  The principle to detect VUR by microwave radiometers is first to warm the bladder with a microwave heating device and control the heating process with a microwave radiometer. The second step is to detect the reflux with an another radiometer at the kidney location. This non-invasive method was conceptually presented by Snow and Taylor [Snow and Taylor, 2010]. Brent W. Snow is the co-founder of Thermimage, Inc.[1] and established a research partnership with Duke University Medical Center in Durham, North Carolina, USA. During my stay at Duke University Medical Center in the academic year 2009-2010, I was invited by Professor Paul Stauffer as a member of the team at Duke University, that worked with development of a non-invasive detection system for VUR [Snow et al., 2011b, Stauffer et al., 2011].

[1] http://www.thermimage.com/

- Microwave radiometry has also been proposed in brain temperature monitoring in newborn infants [Hand et al., 2001, Sugiura et al., 2004]. Cooling of the brain after hypoxia ischaemia may prevent brain damage of infants, but requires temperature measurement at depth in the brain for which invasive methods are not recommended. MRI has been proposed as a measurement method, but turns out to be unsuitable due to the need of repeated temperature measurements over time [Hand et al., 2001]. Instead, a non-invasive multiband microwave radiometer that provides temperature estimates at depth in brain, during brain cooling, is suggested an alternative solution. A complementary brain imaging technique using phased array near field microwave radiometer was also proposed for intracranial applications [Oikonomou et al., 2010,Oikonomou et al., 2009]. Focused microwave radiometry with the use of ellipsoidal conductive wall cavity for human head measurements is an another brain application [Karanasiou et al., 2004a, Karanasiou et al., 2004b].

- Hyperthermia is defined as the delivery of a intended and controlled heat to a disease site without damaging surrounding healthy tissue [Blute and Lewis, 1991]. This is a therapeutic technique in which cancerous tissue is heated to 40-45°C, inducing vascular and cellular changes that improve the therapeutic effectiveness when used in conjunction with chemotherapy or radiation therapy [Wyatt, 2010]. Hence, there is a need of non-invasive temperature quality assurance (QA) of the heated site for controlling power levels of multielement heat applicators, a task that can be obtained by microwave radiometry [Arunachalam et al., 2008].

- Radiometry is also proposed as a non-invasive method to monitor blood glucose for patients with diabetes [Ballew, 2006]. The method can distinguish between changes in the glucose levels, due to variable natural electromagnetic radiation related to this change.

1.3 Organization of the Thesis

Chapter 2 provides an introduction of microwave radiometry. It start with the Black Body radiation and how this is used in a radiometer.
Chapter 3 is an introduction to electrical properties of biological tissues.
Chapter 4 describes the process of designing and building a radiometer.
Chapter 5 gives a short description of the used antenna.
Chapter 6 contain papers 1−5. The papers are described in the next section.
Chapter 7 gives the conclusion and possible future research in the field.

1.4 Included Publications

The following five papers are included in the thesis. The abstract and highlights of the original contributions is given for each paper separately. My contributions in all the papers are based on my inventiveness and of how to implement theoretical and practical knowledge into a new way of solving different problems. In all papers of the thesis, the experimental setups are designed by me.

Paper 1

Ø. Klemetsen, Y. Birkelund, S. K. Jacobsen, P. F. Maccarini and P. R. Stauffer. "**Design of medical radiometer front-end for improved performance**". *Progress In Electromagnetics Research B*, vol. 27, pp. 289-306, 2011.

Abstract– *We have investigated the possibility of building a singleband Dicke radiometer that is inexpensive, small-sized, stable, highly sensitive, and which consists of readily available microwave components. The selected frequency band is at 3.25-3.75 GHz which provides a reasonable compromise between spatial resolution (antenna size) and sensing depth for radiometry applications in lossy tissue. Foreseen applications of the instrument are non-invasive temperature monitoring for breast cancer detection and temperature monitoring during heating. We have found off-the-shelf microwave components that are sufficiently small (< 5mm $\times$ 5mm) and which offer satisfactory overall sensitivity. Two different Dicke radiometers have been realized: one is a conventional design with the Dicke switch at the front-end to select either the antenna or noise reference channels for amplification. The second design places a matched pair of low noise amplifiers in front of the Dicke switch to reduce system noise figure.*

Numerical simulations were performed to test the design concepts before building prototype PCB front-end layouts of the radiometer. Both designs provide an overall power gain of approximately 50dB over a 500MHz bandwidth centered at 3.5GHz. No stability problems were observed despite using triple-cascaded amplifier configurations to boost the thermal signals. The prototypes were tested for sensitivity after calibration in two different water baths. Experiments showed superior sensitivity (36% higher) when implementing the low noise amplifier before the Dicke switch (close to the antenna) compared to the other design with the Dicke switch in front. Radiometer performance was also tested in a multilayered phantom during alternating heating and radiometric reading. Empirical tests showed that for the configuration with Dicke switch first, the switch had to be locked in the reference position during application of microwave heating to avoid damage to the active components (amplifiers and power meter). For the configuration with a low noise amplifier up front, damage would occur to the active components of the radiometer if used in presence of the microwave heating antenna. Nevertheless, this design showed significantly improved sensitivity of measured temperatures and merits further investigation to determine methods of protecting the radiometer for amplifier first front ends.

My contribution in this paper was to find compatible microwave components for the desired frequency band (3.25−3.75 GHz). A previously discovered instability problem of

cascade-coupled amplifiers was initially solved. Further, new designs were developed to minimize the physical size of the front-end. The improvement of these designs, with use of commercial available components, is reduced cost and physical size, compared to a design with connectorized commercial pre-built blocks. The experiment in this paper is novel as controlling of the radiometer and the heating device in a sequential manner that was fully automated. The most important results from this paper are the possibility to use the radiometer in a microwave heating setup, without destroying the radiometer by the high-energy heating signal. Knowledge gained through the experiment on interspersed heating and radiometric temperature reading can be further utilized in hyperthermia treatment for temperature control of the heating process [Stauffer et al., 1998]. Another application is a new device for temperature control of bladder urine prior to vesicoureteral reflux detection [Snow and Taylor, 2010, Snow et al., 2011a, Snow et al., 2011b, Snow, 2011, Arunachalam et al., 2010, Arunachalam et al., 2011].

Paper 2

Ø. Klemetsen, S. K. Jacobsen and Y. Birkelund, "**Radiometric temperature reading of a hot ellipsoidal object inside the oral cavity by a shielded microwave antenna put flush to the cheek**", submitted June 2011, and under review in *Physics in Medicine and Biology*.

Abstract– *A new scheme for detection of vesicoureteral reflux (VUR) in children has recently been proposed in the literature. The idea is to warm bladder urine via microwave exposure to at least fever temperatures, and observe potential urine reflux from the bladder back to the kidneys by medical radiometry. As a preliminary step towards realization of this detection device, we present non invasive temperature monitoring by use of microwave radiometry in adults to observe temperature dynamics in vivo of a water filled balloon placed within the oral cavity. The relevance of the approach with respect to detection of VUR in children is motivated by comparing the oral cavity and cheek tissue with axial CT images of young children in the bladder region. Both anatomical locations reveal a triple-layered tissue structure consisting of skin-fat-muscle with a total thickness of about 8-10 mm. In order to mimic variations in urine temperature, the target balloon was flushed with water coupled to a heat exchanger, that was moved between waterbaths of different temperature, to induce measurable temperature gradients. The applied radiometer has a center frequency of 3.5 GHz and provides a sensitivity (accuracy) of 0.03°C for a data acquisition time of 2 secs. Three different scenarios were tested and included observation through the cheek tissue with and without an intervening water bolus compartment present. In all cases, radiometric readings observed over a time span of 900 secs were shown to be highly correlated ($R \sim 0.93$) with in situ temperatures obtained by fiberoptic probes.*

My contribution in this work was the idea to use a balloon within the human oral cavity to mimic the pediatric bladder, an idea that was conceived from a practical point of view. The intention was to evaluate the radiometer design in an *in-vivo* experiment

without surgical intervention. The idea originated from the work in the scientic group at Duke University Medical Center, where we worked on the vesicoureteral reflux (VUR) detection problem. The results from this paper provide a step forward to develop a safe and working device to detect VUR. The datasets were generated with me as a volunteer.

Paper 3

Ø. Klemetsen and S. Jacobsen, "**Improved Radiometric Performance Attained by an Elliptical Microwave Antenna With Suction**", accepted in *IEEE Transactions on Biomedical Engineering*". 2011 Oct 18. [Epub ahead of print]

Abstract– *We present a new way to securely mount a medical microwave antenna onto the human body for improved in-vivo temperature measurements by microwave radiometry. A low cost and simple vacuum pressure source is used to provide suction (negative pressure) on the aperture of an elliptical antenna with vacuum chamber cavity backing. The concept offers improved electromechanical coupling between the antenna surface and the skin of the body. The proposed solution is evaluated experimentally to test repeatability of radiometric temperature measurements by remounting the antenna many times in one sequence on a given anatomical location. Four representative locations (hand, belly, hip and chest) were used to test the suction antenna concept against anatomical curvature and load variations. Statistical analysis shows a marked decrease in the standard deviation of the measured temperatures with use of suction compared to conventional manual fixation. At repeated measurements, the vacuum antenna produces less uncertainty and improved estimate of the true lossy load temperature. During body movement, the antenna mounted at bone-filled areas shows greatest potential for improved performance.*

After an animal experiment in Salt Lake City (the results from this experiment is described in the literature [Snow et al., 2011a]) I saw the need to properly mount an antenna *in-vivo* for better coupling to the human skin. My idea was to use negative pressure to mount and maintain an antenna in a given position. The result from this experiment is a solution to a practical problem in many fields where you have to mount an antenna directly onto the object under investigation. It could either be used for an active or a passive antenna setup or a combination of both principles. The datasets in this paper were obtained with me as the experimental volunteer.

Paper 4

Yngve Birkelund, Øystein Klemetsen, Svein K. Jacobsen, Kavitha Arunachalam, Paolo Maccarini, and Paul R. Stauffer. "**Vesicoureteral reflux in children: A phantom study of microwave heating and radiometric thermometry of pediatric bladder**", *IEEE Transactions on Biomedical Engineering*, vol. 58 no. 11, pp 3269-3278, November 2011.

Abstract– *We have investigated the use of microwave heating and radiometry to safely heat urine inside a pediatric bladder. The medical application for this research is to create a safe and reliable method to detect vesicoureteral reflux, a pediatric disorder, where urine flow is reversed and flows from the bladder back up into the kidney. Using fat and muscle tissue models, we have performed both experimental and numerical simulations of a pediatric bladder model using planar dual concentric conductor microstrip antennas at 915 MHz for microwave heating and a planar elliptical antenna connected to a 500 MHz bandwidth microwave radiometer centered at 3.5 GHz for non-invasive temperature measurement inside tissue. Temperatures were measured in the phantom models at points during the experiment with implanted fiberoptic sensors, and 2D distributions in cut planes at depth in the phantom with an infrared camera at the end of the experiment. Cycling between 20 second with 20 Watts power for heating, and 10 seconds without power to allow for undisturbed microwave radiometry measurements, the experimental results show that the target tissue temperature inside the phantom increases fast and that the radiometer provides useful measurements of spatially averaged temperature of the illuminated volume. The presented numerical and experimental results show excellent concordance, which confirms that the proposed system for microwave heating and radiometry is applicable for safe and reliable heating of pediatric bladder.*

My contribution in this paper is the radiometer hardware which I designed and built from scratch. The experimental setup with control of the radiometer and heating device is designed by me, and I have also been involved in most of the practical experiments.

Paper 5

Jacobsen, Svein Ketil; Klemetsen, Øystein. "**Improved Detectability in Medical Microwave Radio-Thermometers as Obtained by Active Antennas**", *IEEE Transactions on Biomedical Engineering*, vol. 55, no. 12, pp. 2778-2785, December 2008.

Abstract– *Microwave radiometry is a spectral measurement technique for resolving blackbody radiation of heated matter above absolute zero. The emission levels vary with frequency and are at body temperatures maximized in the infrared spectral band. Medical radio-thermometers are mostly noninvasive short-range instruments that can provide temperature distributions in subcutaneous biological tissues when operated in the microwave region. However, a crucial limitation of the microwave radiometric observation principle is the extremely weak signal level of the thermal noise emitted by the lossy material (-174 dBm/Hz at normal body temperature). To improve the radiometer SNR, we propose to integrate a tiny, moderate gain, low-noise preamplifier (LNA) close to the antenna terminals as to obtain increased detectability of deep seated thermal gradients within the volume under investigation. The concept is verified experimentally in a lossy phantom medium by scanning an active antenna across a thermostatically controlled water phantom with a hot object embedded at 38 mm depth. Three different setups were investigated with decreasing temperature contrasts between the target and ambient medium. As a direct consequence of less ripple on the raw radiometric signal, statistical analysis shows a marked*

increase in signal-to-clutter ratio of the brightness temperature spatial scan profiles, when comparing active antenna operation with conventional passive setups.

My contribution in this paper is the experimental setup with the idea and design of the miniature Faraday cage with use of waveguides to avoid incoming interference. The center frequency of this radiometer setup was 1.57 GHz and thus more suspended to electro-magnetic interference then the later selected 3.5 GHz band. The pre-amplifier is built and tested by me. The idea to use a monopole antenna is mine, and most of the datasets in the experiments were generated by me.

1.5 Other Publications and Presentations

As First Author:

1. Ø. Klemetsen, Y. Birkelund, P. F. Maccarini, K. Arunachalam, V. De Luca, S. K. Jacobsen and Paul R. Stauffer. "**Miniature radiometer frontend design for non-invasive temperature measurements**", Poster Presentation in *Society for Thermal Medicine 2010 Annual Meeting*, (Florida, USA), April 23 - 26, 2010.

2. Ø. Klemetsen, Y. Birkelund, P.F. Maccarini, P. Stauffer and S.K. Jacobsen. "**Design of Small-sized and Low-cost Front End to Medical Microwave Radiometer**", Oral Presentation in *PIERS Proceedings*, (Cambridge, USA), July 5-8, 2010.

3. Ø. Klemetsen, Y. Birkelund and S. Jacobsen. "**Low-cost and small-sized medical microwave radiometer design**", Oral Presentation in *IEEE Antennas and Propagation Society International Symposium (APSURSI)*, (Toronto, Canada), July 11-17, 2010.

4. Øystein Klemetsen and Svein Jacobsen. "**Improved Radiometer Reading with a Moderate Negative Pressure Microwave Antenna**", in *IEEE Applied Electromagnetics Conference AEMC and Indian Antenna Week IAW*,(Kolkata, India), Desember 18-22, 2011, accepted for "Student Paper Contest [SPC]".

5. Øystein Klemetsen, Svein Jacobsen and Yngve Birkelund. "**Improved Radiometer Temperature Reading with Suction on the Antenna**", in *The 3rd Norwegian PhD Conference in Medical Imaging*, (Oslo, Norway), November 21-22, 2011. Invitated to poster presentation.

As Coauthor:

1. Jacobsen, Svein Ketil; Klemetsen, Øystein. "**Active antennas in medical microwave radiometry**", *Electronics Letters*, vol. 43, pp. 606-608, May 2007.

2. Jacobsen, Svein Ketil; Klemetsen, Øystein. "**Implementation of Active Antennas in Medical Microwave Radio-Thermometry**", in *Progress in Electromagnetics Research Symposium (PIERS)*, (Prague, Czech Republic), August 26-30, 2007.

3. Y. Birkelund, Ø. Klemetsen, K. Arunachalam, V. De Luca, P. F. Maccarini, S. K. Jacobsen and P. R. Stauffer, "**Radiometric temperature monitoring of microwave hyperthermia**", in *Society for Thermal Medicine 2010 Annual Meeting*, (Florida, USA), April 23 - 26, 2010.

4. Stauffer, Paul R.; Maccarini, Paolo; Arunachalam, Kavitha; De Luca, Valeria; Klemetsen, Øystein; Birkelund, Yngve; Jacobsen, Svein Ketil; Bardati, F; Tognolatti, P; Snow, Brent W.. "**Non-Oncologic Application for Microwave Radiometry in Temperature Monitoring and Control**", in *26th Annual Meeting of European Society for Hyperthermic Oncology*, (Rotterdam, The Netherlands), May 20-22, 2010.

5. B. W. Snow, P. R. Stauffer, K. Arunachalam, P. Maccarini, V. De Luca, Ø. Klemetsen and Y. Birkelund. "**Non-Invasive Vesicoureteral Reflux Detection: A New Device**", in *American Academy of Pediatrics National Conference and Exhibition* (California, USA), October 1 - 5, 2010.

6. Paul R. Stauffer, Paolo F. Maccarini, Valeria De Luca, Sara Salahi, Alina Boico, Kavitha Arunachalam, Øystein Klemetsen, Yngve Birkelund, Svein K. Jacobsen, Fernando Bardati, Piero Tognolotti and Brent Snow. "**Microwave radiometry for non-invasive detection of vesicoureteral reflux (VUR) following bladder warming** ", Invited Paper in *Society of Photo-Optical Instrumentation Engineers (SPIE)*, (San Francisco, California, USA), January 22-27, 2011.

7. B. W. Snow, K. Arunachalam, V. De Luca, Ø. Klemetsen, Y. Birkelund, P. R. Stauffer, and P. Maccarini. "**Noninvasive Grade V Vesicoureteral Reflux Detection: An Animal Study**", in *22nd Annual Congress of the ESPU*, (Copenhagen, Denmark), April 27-30, 2011.

8. B. W. Snow, K. Arunachalam, V. De Luca, Ø. Klemetsen, Y. Birkelund, P. R. Stauffer, and P. Maccarini. "**Noninvasive Grade V Vesicoureteral Reflux Detection: An Animal Study**", in *The Internet Journal of Urology*, vol. 185, pp. e232-e232, April 2011.

9. Snow BW, Arunachalam K, De Luca V, Maccarini PF, Klemetsen Ø, Birkelund Y, Pysher TJ, and Stauffer PR. "**Non-invasive vesicoureteral reflux detection: Heating risk studies for a new device**", article in press *Journal of Pediatric Urology*, 2011.

10. Paolo Maccarini, Paul Stauffer, Sara Salahi, Alina Boico, Øystein Klemetsen, Yngve Birkelund, Valeria De Luca, Kavitha Arunachalam and Brent Snow. "**A Novel Ultrasensitive Microwave Radiometer for Noninvasive Subsurface Temperature Measurements**" in *Society for Thermal Medicine 2011 Annual Meeting*, (New Orleans, USA), April 29 - May 2, 2011.

11. Paul Stauffer, Paolo Maccarini, Kavitha Arunachalam, Valeria De Luca, Sara Salahi, Alina Boico, Øystein Klemetsen, Yngve Birkelund, Svein Jacobsen, Fernando Bardati, Piero Tognolatti and Brent Snow. "**Radiometric Monitoring of Kidneys During Bladder Warming for Non-Invasive Detection of Vesicoureteral Reflux (VUR)**", in *Society for Thermal Medicine 2011 Annual Meeting*, (New Orleans, USA), April 29 - May 2, 2011.

12. B. Snow, K. Arunachalam, V. De Luca, Ø. Klemetsen, Y. Birkelund, P. Stauffer and P. Maccarini. "**Noninvasive Grade V Vesicoureteral Reflux Detection: An Animal Study**", in *AUA Annual Meeting*, (Washington DC, USA), May 14-19, 2011.

Chapter 2

Radiometry

Radiometry is a completely non-invasive, non-toxic and relatively inexpensive sensing modality. The radiometric technique is based on the measurement of electromagnetic noise power emitted by lossy materials. The greatest intensity of radiation comes from the infrared (IR) spectrum when we look at human body temperatures (310 K). Because of high attenuation of infrared waves in tissues, IR radiometry is limited to the measurement of surface temperature of human tissue [Stec et al., 2004].

On the other hand, in the microwave range the intensity is about *10 million* (-70 dBW) times smaller in comparison to infrared radiation. Nevertheless, microwave radiation is less attenuated in tissue, and is therefore suitable for measuring the temperature subcutaneously. In the microwave range, the emission of radiation from an object is proportional to the temperature of the object [Ulaby et al., 1981, Stec and Susek, 2000, Ulaby et al., 1986]. Therefore, by positioning a connected microwave antenna at an anatomical site, an existing temperature gradient at depth can be detected if the temperature difference is above the given temperature sensitivity threshold of the radiometer. On this basis, we will further look into the theory behind microwave radiometry.

2.1 Black Body Radiation

Thermal energy is kinetic energy of random particle motion in a material. The concentration of energy in an object is quantified by its temperature. The random motion of particles is a result of collisions between particles and interfaces. Further, cause of collisions is a change in the path of an electron or vibration and rotation of a molecule or atom. Energy conditions induced by collisions can spontaneously change from a high to a low energy level. This results in a spontaneous emission of electromagnetic waves. In this way, thermal energy is connected to the radiation energy [Reeves et al., 1975, Leroy et al., 1998]. The spectrum of thermal radiation from a body is continuous and spreads over all wavelengths. A quantitative description of energy distribution across different wavelengths is given by the spectral emittance [Ohanian, 1985]. This quantity is defined as the energy flux emitted from the surface of an object per unit wavelength. An ideal

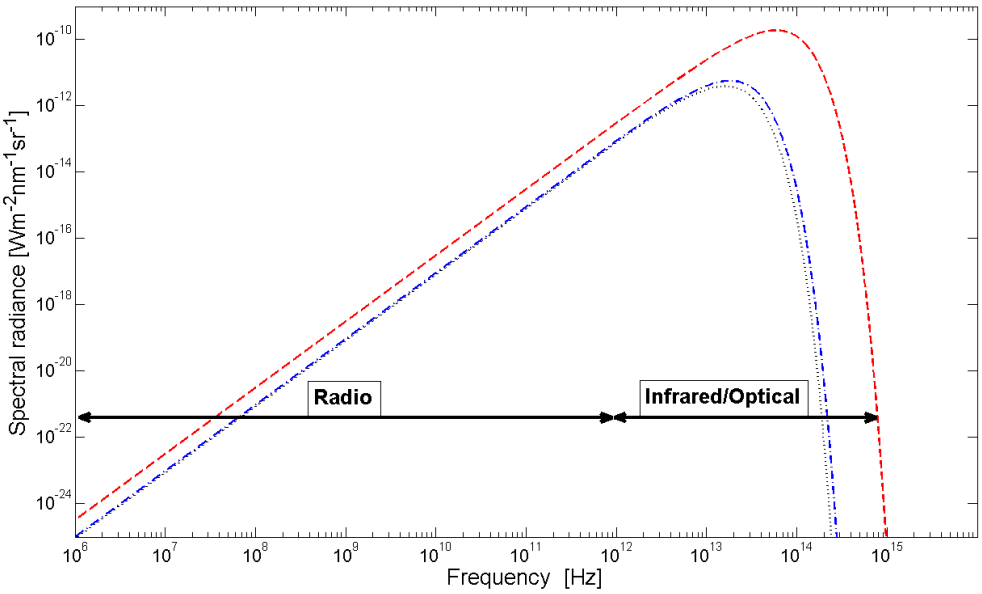

Figure 2.1: Black body radiation at 273 K (black line), 310 K (blue line) and 1000 K (red line) for the radio and infrared/optical frequencies.

thermal emitter is defined as a "black body". Such an object transforms thermal energy to radiation energy in accordance on the second law of thermodynamics. The opposite situation is also the case, i.e. the ability to transform radiant energy into heat energy.

2.1.1 Planck's Law

In 1900, Max Planck formulated the spectral radiation from a black body. Emission per unit frequency, as a function of f, is given by:

$$B_f(f) = \frac{2hf^3}{c^2} \frac{1}{e^{\frac{hf}{kT}} - 1}, \tag{2.1}$$

where c is the speed of light, h is Planck's constant, k is Boltzmann's constant, T is the temperature and B_f is the spectral radiance. An illustration of spectral radiance at different temperatures versus frequency is given in figure 2.1. Note that the intensity in the infrared range is many orders of magnitude (10^7) higher than in the microwave range, i.e. from 1 to 10 GHz [Leroy et al., 1987].

2.1.2 Rayleigh-Jean's Approximation

Planck's law can be approximated by Rayleigh-Jean's law in the microwave frequency range through Taylor series expansion of the exponential term ($e^{hf/kT} - 1 \simeq \frac{hf}{kT}$) and under the assumption that $hf \ll kT$ [Reeves et al., 1975, Pozar, 1998]:

$$B_f(f) = \frac{2kTf^2}{c^2}. \tag{2.2}$$

Eq. (2.2) has an accuracy of 1% when $f/T < 3.9 \times 10^8$ Hz/K. If one assumes a body temperature of 310 K in eq. (2.2), the Rayleigh-Jean's approximation is valid for frequencies $f < 121$ GHz. This means that Rayleigh-Jean's law can be used for microwave radiometry modeling in the frequency range common in microwave radiometry.

2.1.3 Nyquist Law

It can be shown that Rayleigh-Jean's approach leads to the Nyquist law [Ulaby et al., 1981]. This gives the noise power P, transmitted to a radiometer antenna that is connected to a material with absolute temperature T. The power density is uniformly distributed in the microwave spectrum and for a bandwidth B, accumulates to a total power given by [Ulaby et al., 1981, Leroy et al., 1998]:

$$P = kTB. \tag{2.3}$$

It is interesting to observe: As $B \to \infty$ then $P \to \infty$. This is the "*ultraviolet catastrophe*", which is not a physical reality, because eqs. (2.2)-(2.3) are not valid and we have to use eq. (2.1) instead. Further, if $B \to 0$ then $P \to 0$ and if $T \to 0$ then $P \to 0$.

Emissivity ϵ is the relation between radiation from a real body and the theoretical maximum radiation given by Planck's law [Reeves et al., 1975, Pozar, 1998]. Emissivity is a normalized constant with value between 0 and 1, and is a function of the object's dielectric constant, surface structure, temperature, wavelength and viewing angle [Zwally, 1977, Ulaby et al., 1981]. Emissivity can be expressed as, $\epsilon = 1 - |\rho|^2$ with $|\rho|^2$ defined as the power reflection coefficient at the antenna terminals [Dubois et al., 1996, Larsi et al., 1999]. The brightness temperature T_B can be expressed in term of emissivity as $T_B = \epsilon T$, where T is the physical temperature of a body with homogeneous temperature. Hence, the antenna power P_A with a brightness temperature T_B is $P_A = kT_BB$.

2.2 Principles of Radiometers

Radiometers have constructions similar to receivers used in communication, radar and wireless local area network (WLAN). The most common system is the superheterodyne receiver, that uses a local oscillator (LO) and a frequency mixer to down convert the high frequency (HF) band to a lower intermediate-frequency (IF), before the signal is amplified in the IF amplifier, demodulated and then amplified in the low frequency (LF) amplifier. It is customary to denote radiometer front-end as the typically high frequency section (including IF) while the back-end is from the detector and rest of the electronic components.

Many radiometer types have been investigated in the literature [Gunnarsson et al., 2008, Land, 2001, Skou and Vine, 2006, Dubois et al., 1996, Goodberlet and Mead, 2006, Dubois et al., 2000]. Theoretical and practical studies have been performed for different applications.

2.2.1 Radiometer Sensitivity

The most important characteristic of the radiometer system is sensitivity [Sharkov, 2003], defined as the minimum signal threshold that can be detected. The signal of interest has to be above this limit. The sensitivity of a radiometer is heavily dependent on the radiometer design.

Figure 2.2 illustrates an idealized and a real total power radiometer. In the idealized case, the output power is $P = kGBT_A$, where G is the gain in the radiometer receiver and the radiometer is assumed noiseless. To illustrate the sensitivity challenge, the real radiometer generates internal noise that will add to the input signal, and this equivalent noise temperature T_E has the same nature as the antenna input noise T_A. Hence, the output in the real case is $P = kGB(T_A + T_E)$.

The radiometer sensitivity can be described as the standard deviation of the output power. The stochastic input signal to the radiometer is modeled as having zero mean with a variance related to the temperature. If the input noise signal of bandwidth B is integrated over a time τ, the variance is reduced by a factor of $B\tau$. The variance can thus be described by:

$$\sigma^2 \cong \frac{P^2}{B\tau}, \tag{2.4}$$

and the standard deviation as σ if the square root is applied on eq. (2.4). The standard deviation or sensitivity of the output is then [Tiuri, 1964, Ulaby et al., 1981]:

$$\Delta T_{\mathtt{min}} = \frac{(T_A + T_E)}{\sqrt{B\tau}}, \tag{2.5}$$

where τ is the integration time in the lowpass filter of the radiometer. This basic sensitivity formula has to be taken into account in performance considerations of radiometers.

2.2.2 Total Power Radiometer

A total power radiometer is the simplest radiometer type and a block diagram is shown in figure 2.3. The principle is to connect an antenna to a broadband amplifier with low noise. Thereafter, the superheterodyne principle is used to detect the noise signal in a square law detector to produce a mean value direct current (DC) voltage superimposed on a fluctuating high frequency component. The last stage is integration to perform lowpass filtering of the DC signal in an integrator with time constant τ. The proportional output voltage from the radiometer is then:

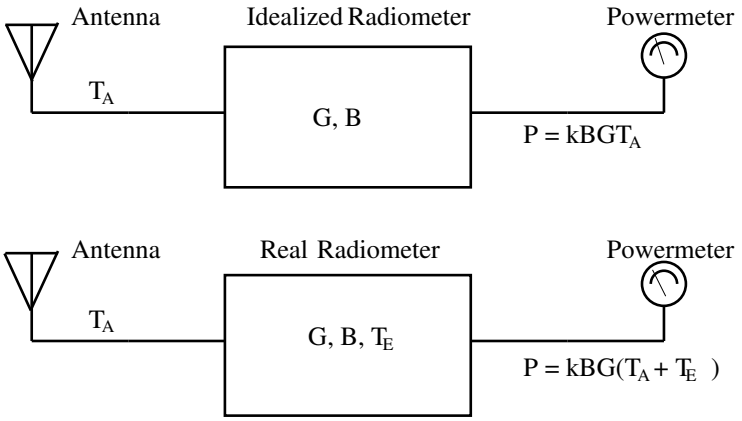

Figure 2.2: Idealized and real total power radiometer.

$$V_{\mathtt{OUT}} = kGB(T_A + T_E)C, \tag{2.6}$$

where G is the overall gain and C is the sensitivity of the square law detector given in V/W. The sensitivity of the total power radiometer is given in eq. (2.5) and is the standard deviation of the random noise temperature. An important and more serious source of measurement error is gain drift in the radiometer amplifier stages. The RMS time dependent gain drift ΔG of the total gain G contributes to a temperature measurement error:

$$\Delta T_G = (T_A + T_E)\frac{\Delta G}{G}. \tag{2.7}$$

The overall temperature measurement error in a total power radiometer is thus given by:

$$\Delta T = \sqrt{(\Delta T_{\mathtt{min}})^2 + (\Delta T_G)^2}. \tag{2.8}$$

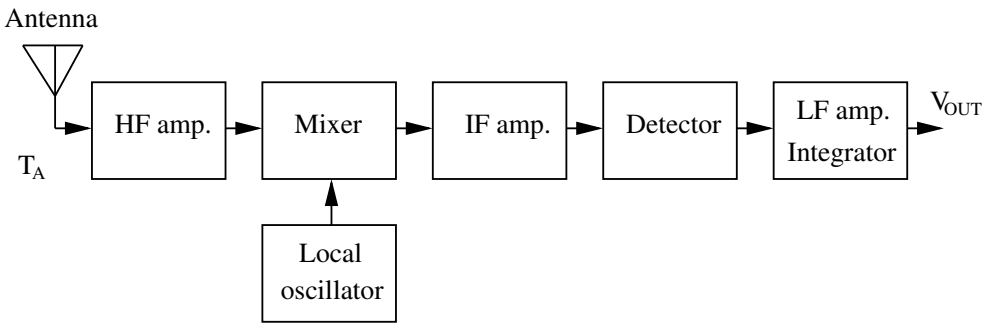

Figure 2.3: Total power radiometer.

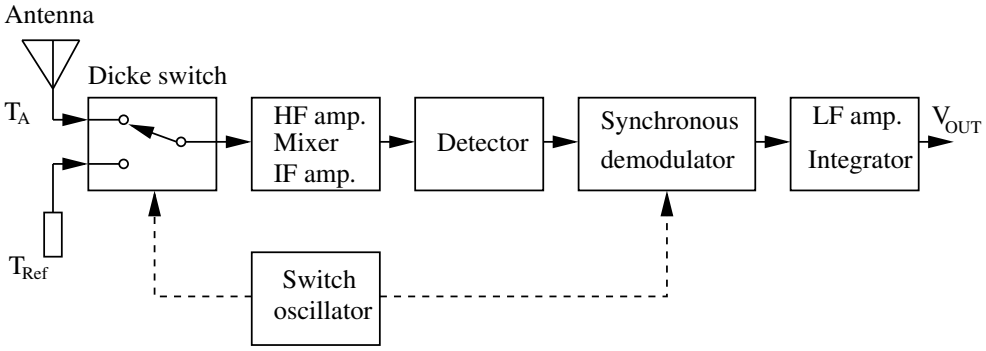

Figure 2.4: Dicke radiometer.

2.2.3 Dicke Radiometer

The optimum device to receive noise-type signals consists of an ideal and noiseless amplifier, square law detector and an integrator. The gain fluctuations ΔG in the total power radiometer are slow in time, but contribute to a large measurement error. If we are able to calibrate the radiometer with a higher rate then the rate of the gain fluctuations, the overall measurement error can be reduced significantly. This idea was used in a radiometer design developed by R.H. Dicke in 1946. Figure 2.4 illustrates his idea and the concept is called a Dicke radiometer. The modulation principle to eliminate the radiometer instabilities is to switch between the antenna (T_A) and a reference load ($T_{\mathtt{Ref}}$) with a repetition frequency $f_{\mathtt{Mod}}$. If $f_{\mathtt{Mod}}$ is high enough in comparison with the inverse gain fluctuation time constant, it is possible to detect a signal of interest without being affected by gain fluctuations. The signal is demodulated in a synchronous demodulator controlled by the switching frequency $f_{\mathtt{Mod}}$. The modulation frequency $f_{\mathtt{Mod}}$ is in the range from 10-1000 Hz and should not be a multiple of the power line frequency (50 Hz) to avoid interference. The voltages from the square law detector are $V_1 = kGB(T_A + T_E)C$ when the switch is in the antenna position and $V_2 = kGB(T_{\mathtt{Ref}} + T_E)C$ in the reference switch position. The output voltage from the synchronous demodulator is the difference between the reference load and the antenna:

$$V = kGB(T_A - T_{\mathtt{Ref}})C. \tag{2.9}$$

If $T_A = T_{\mathtt{Ref}}$, output voltage fluctuations due to gain variations disappear and the sensitivity of the Dicke radiometer is given:

$$\Delta T_{\mathtt{min,Dicke}} = 2\frac{(T_A + T_E)}{\sqrt{B\tau}}. \tag{2.10}$$

Note that the sensitivity of the Dicke radiometer is twice of the sensitivity of the total power radiometer, since the antenna is connected half of the time and the remaining time measuring the reference temperature. In general $T_A \neq T_{\mathtt{Ref}}$ because it is difficult to produce a reference temperature to follow the antenna temperature completely. Hence, other principles has been implemented to obtain this requirement. These solutions are

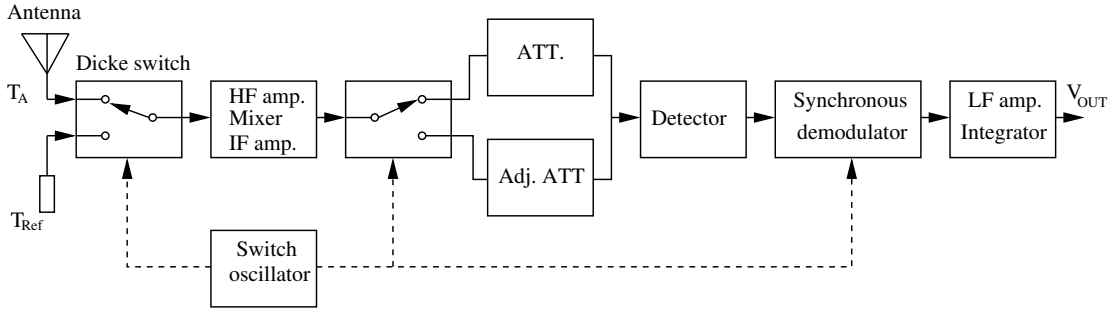

Figure 2.5: Gain modulated Dicke radiometer.

presented in the next sections. The sensitivity of the Dicke radiometer in its most general form is given by [Ulaby et al., 1981]:

$$\Delta T_{\mathtt{Dicke}} = \left[\frac{2(T_A + T_E)^2 + 2(T_{\mathtt{Ref}} + T_E)^2}{B\tau} + \left(\frac{\Delta G}{G} \right)^2 (T_A - T_{\mathtt{Ref}})^2 \right]^{1/2} . \tag{2.11}$$

However, if $T_A \approx T_{\mathtt{Ref}}$, the last term in eq. (2.11) can be neglected.

2.2.4 Gain Modulated Dicke Radiometer

As mentioned above, $T_A \neq T_{\mathtt{Ref}}$ in many measurement cases. To obtain $T_A \approx T_{\mathtt{Ref}}$, a gain modulated Dicke design is one option and is depicted in figure 2.5. The idea is to use another switch and two attenuators, one fixed and one adjustable. The adjustable attenuator is used to balance one of the radiometer channel to obtain $T_A \approx T_{\mathtt{Ref}}$, and hence a improved sensitivity.

2.2.5 Null Balancing Dicke Radiometer

An automatic adjustment of $T_{\mathtt{Ref}}$ such that $T_A = T_{\mathtt{Ref}}$ is preferable. This requirement is the basis for the null balancing Dicke radiometer, which is illustrated in figure 2.6. A controllable noise generator is used for $T_{\mathtt{Ref}}$ and is controlled by a feedback loop to obtain $T_A = T_{\mathtt{Ref}}$. If the design is working properly, the sensitivity is as described in eq. (2.10). The reference noise generator can be made of a 50 Ω load that is temperature controlled or an active noise generator.

2.2.6 Graham's Radiometer

Graham presented in 1958 a new way to increase the sensitivity by use of two radiometers that is switched in a special manner. The net result is an increase in sensitivity by a factor of $\sqrt{2}$ [Tiuri, 1964]. However, the price to be paid for this is the necessity of two radiometer chains as well as the extra input and output circuits. The principle is illustrated in figure 2.7.

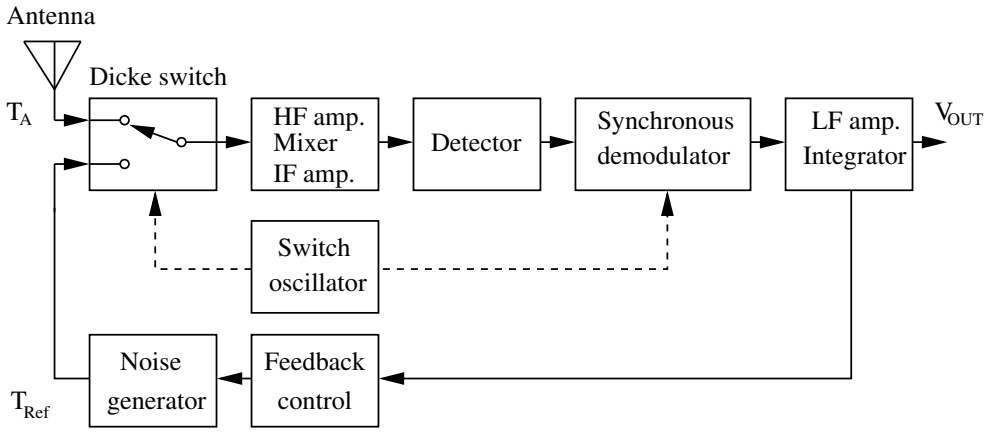

Figure 2.6: Null balancing Dicke radiometer.

2.2.7 Correlation Radiometer

The correlation radiometer consists of two radiometer chains with separate antennas (see figure 2.8). The idea is to measure two brightness temperatures as well the correlation between them. Both antennas are looking at the same signal source. The correlation part is realized in a complex hardware correlator providing the imaginary and real parts of the cross correlation between the two radiometer chains. The output from the two total power chains has a sensitivity that is similar to total power radiometers. However, the correlation outputs have a sensitivity that is a factor $\sqrt{2}$ better than the sensitivity for the total power radiometer. The stability of this radiometer is better than for a total power radiometer, since the internally noise processes in the two radiometer parts is uncorrelated and thus do not contribute to the output of the correlator [Fujimoto, 1964, Tiuri, 1964, Skou and Vine, 2006].

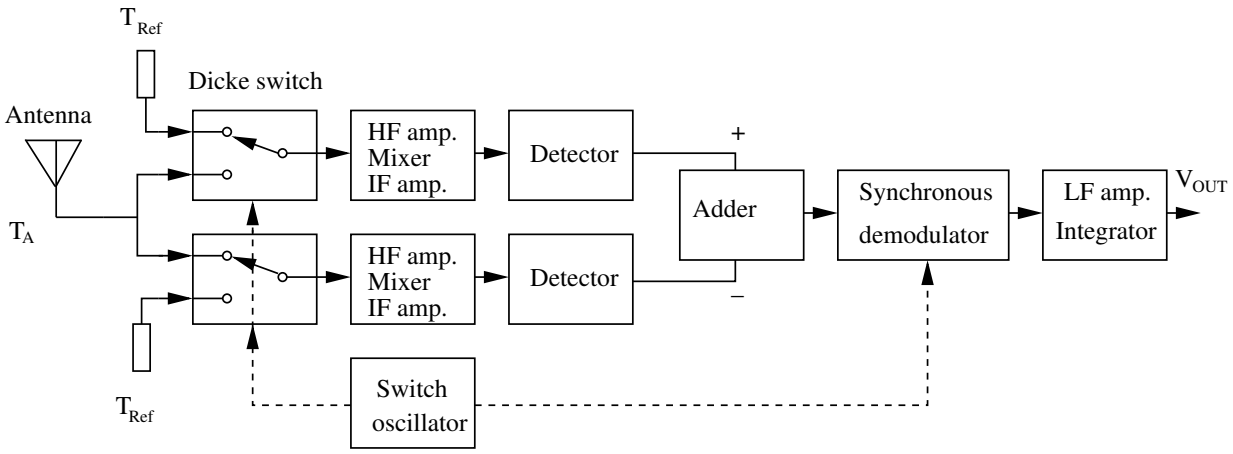

Figure 2.7: Graham's radiometer.

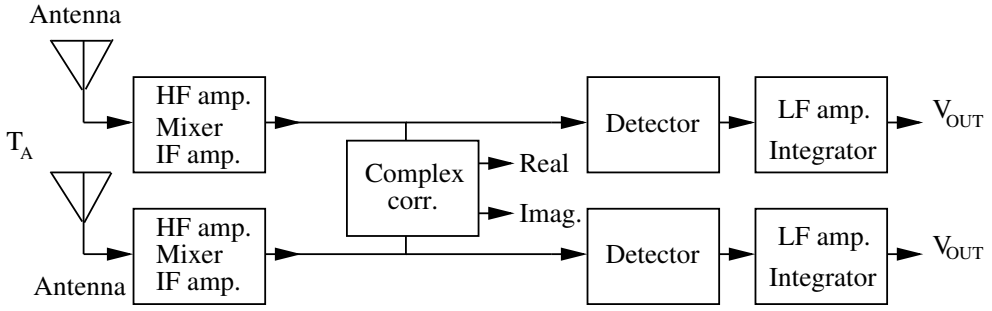

Figure 2.8: Correlation radiometer.

2.3 The Radiometric Equation

The brightness temperature T_B measured by the radiometer is the sum of the weighted volume average of the tissue temperature and is described by the radiometric equation [Jacobsen and Stauffer, 2002]:

$$T_B = (1-\rho)\int_V W(\underline{r})\,T(\underline{r})\,\mathrm{d}V + (1-\rho)\,T_{EMI} + T_E, \tag{2.12}$$

where T_B is the brightness temperature of the object under investigation, ρ is the power reflection coefficient, $W(\underline{r})$ is the radiometric weighting function, $T(\underline{r})$ is the spatial temperature of the object at the position $\underline{r}$, T_{EMI} is the electromagnetic interference and T_E is the equivalent noise temperature in the radiometer system.

The radiometric weighting function is given by

$$W(\underline{r}) = \frac{\sigma_m|\underline{E}(\underline{r})|^2}{\int_V \sigma_m|\underline{E}(\underline{r})|^2\mathrm{dV}}, \tag{2.13}$$

where $\underline{E}$ is the electric field intensity of a lossy medium and σ_m is the medium conductivity for a specific frequency with all terms of loss included. The radiometric weighting function is normalized according to [Reeves et al., 1975]

$$\int_V W(\underline{r})\mathrm{d}V \equiv 1. \tag{2.14}$$

From eq. (2.12) it is interesting to observe that the estimate of the brightness temperature is increased if the equivalent noise temperature in the radiometer system decreases.

Reduction of EMI produce a more accurate estimate of the brightness temperature. This can be shown by rewriting eq. (2.12) to:

$$T_B - (1-\rho)\,T_{EMI} = (1-\rho)\int_V W(\underline{r})\,T(\underline{r})\,\mathrm{d}V + T_E, \tag{2.15}$$

because the EMI produces a bias to the brightness temperature as seen by the second term. If the radiometer and the antenna system is properly shielded from EMI, T_{EMI}

can be neglected in eq. (2.15). Hence the brightness temperature is then given by:

$$T_B = (1 - \rho) \int_V W(\underline{r})\, T(\underline{r})\, \mathrm{d}V + T_E. \tag{2.16}$$

Further, contribution from T_E to T_B in eqs. (2.12) and (2.16) can be handled by proper calibration of the system.

Chapter 3

Dielectrical Properties of Biological Media

When studying the interaction of electromagnetic waves with the human body, it is imperative to understand the electromagnetic properties of the body tissues [Campbell and Land, 1992]. The human body is a complex and stratified dielectric object and it is challenging to characterize the dielectrical properties, because the parameters depend on the frequency and the polarization of the applied electromagnetic field.

3.1 Electromagnetic Properties of Human Tissues

Biological substances are comprised mostly of water that constitutes 72% of the human body. Typically, 99% of the tissue mass are made of four elements; hydrogen, carbon, nitrogen and oxygen [Sprawls, 1987]. Different biological tissues have different water contents, and a key measurement parameter of microwave properties is the dielectric constant or permittivity, that is directly related to water content. The permittivity explains the material loss characteristics and ability to store energy when the material is placed in an electric field [Sprawls, 1987]. Water molecules attempt to align themselves within an electric field, because of their polar nature.

3.2 Permittivity

The permittivity of biological tissues is determined by several important dispersion phenomena whose contributions are normally confined to specific frequency bands. However, the permittivity ε describes how the alignment mentioned above is achieved and is the ratio between the displacement flux $\bar{D}$ and electric field $\bar{E}$, $\varepsilon = \bar{D}/\bar{E}$ [Pozar, 2004]. Human body tissues are in general lossy materials. A lossy material has a complex valued permittivity $\varepsilon = \varepsilon' - j\varepsilon''$ for a given frequency, where the imaginary part of ε accounts for loss in the material due to damping of the vibrating dipole moments,

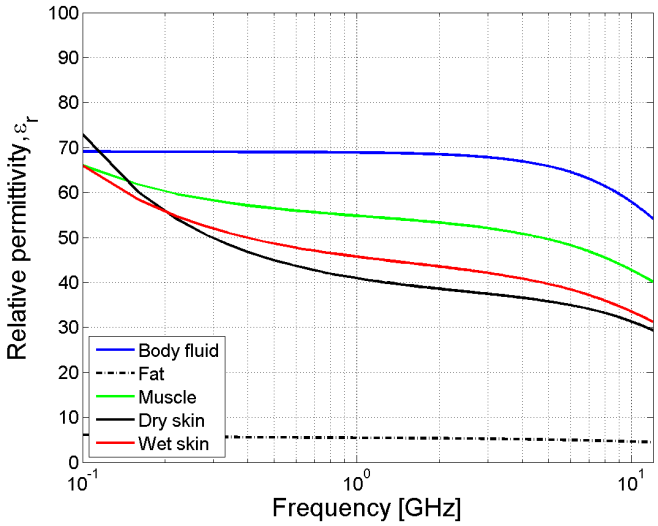

Figure 3.1: Relative permittivity versus frequency for some body materials [IFAC, 2011].

and $\varepsilon' = \varepsilon_r \varepsilon_0$ where ε_r is the dielectric constant of the material and ε_0 is the permittivity of free space [Pozar, 2004]. The relative permittivity ε_r is depicted in figure 3.1 for some biological tissues as a function of frequency. The complex relative permittivity (ε) and its frequency dependency is often modeled by the Debye equation [Gabriel et al., 1996]:

$$\varepsilon(\omega) = \varepsilon_\infty + \frac{\varepsilon_s - \varepsilon_\infty}{1 + \mathrm{j}\omega\tau_\mathrm{r}}, \tag{3.1}$$

where ε_s and ε_∞ are the low and high frequency limits of the dielectric constant, respectively. ω is the angular frequency of the applied field and τ_r is the relaxation time. Eq. (3.1) can be splitted into real and imaginary parts:

$$\varepsilon'(\omega) = \varepsilon_\infty + \frac{\varepsilon_s - \varepsilon_\infty}{1+\omega^2\tau_r^2} \tag{3.2a}$$

$$\varepsilon''(\omega) = \frac{(\varepsilon_s - \varepsilon_\infty)\omega\tau_r}{1+\omega^2\tau_r^2}. \tag{3.2b}$$

Tissue materials are a composition of biological materials with different frequency dependence (dispersion) regions. However, the complexity of both structure and composition of the material is such that each region with dispersion may be broadened [Gabriel et al., 1996, Hurt, 1985]. The broadening is due to multiple contributions to the dispersion region. This broadening can be empirically accounted for by introducing a parameter, called distribution parameter α, giving an alternative to the Debye equation, the so-called Cole-Cole equation:

$$\varepsilon(\omega) = \varepsilon_\infty + \frac{\varepsilon_s - \varepsilon_\infty}{1 + (\mathrm{j}\omega\tau_\mathrm{r})^{1-\alpha}}. \tag{3.3}$$

A multiple Cole-Cole dispersion can be expressed by generalizing eq. (3.3) to:

$$\varepsilon(\omega) = \varepsilon_\infty + \sum_n \frac{\Delta\varepsilon_n}{1 + (\mathrm{j}\omega\tau_{\mathrm{r,n}})^{1-\alpha_\mathrm{n}}} + \frac{\sigma_i}{\mathrm{j}\omega\varepsilon_0}, \tag{3.4}$$

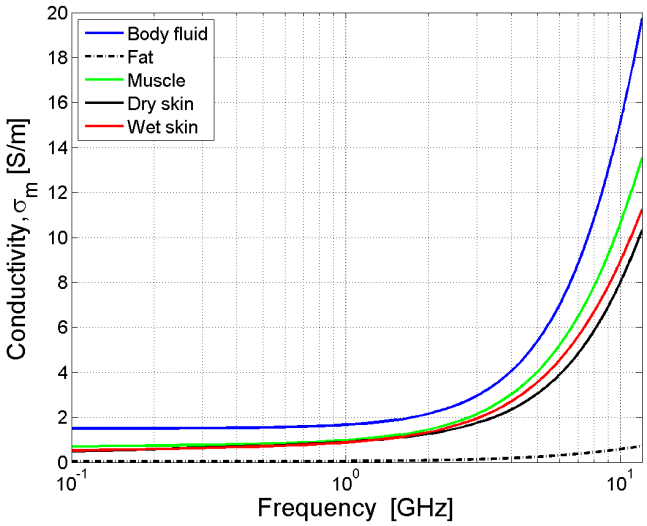

Figure 3.2: Conductivity versus frequency for some body materials [IFAC, 2011].

where $\Delta\varepsilon = \varepsilon_s - \varepsilon_\infty$ and σ_i is the static ionic conductivity. With a proper choice of parameters appropriate for each material, eq. (3.4) can be used to model the dielectric properties over a given frequency range.

3.3 Conductivity

The conductivity values for a given frequency in the material is denoted σ_m, a σ_m is illustrated in figure 3.2 for some biological tissues. Debye relaxation equation can also estimate the conductivity by [Campbell and Land, 1992]:

$$\sigma_m = \frac{\varepsilon_0(\varepsilon_s - \varepsilon_\infty)\omega^2\tau_r}{1 + \omega^2\tau_r^2}. \tag{3.5}$$

The dielectric properties of tissue are determined by a number of dispersion phenomena that is frequency dependent. Microwave frequencies used in this thesis is within the γ-dispersion region [Sha et al., 2002, Formica and Silvestri, 2004]. The dielectric properties of tissues above 100 MHz are determined by the intra-cellular electrolytes, principally water. These properties are consistent with those from suspensions of low conductivity. In the microwave frequency band, tissue properties can be attributed to their *free* water content and the dispersion for normal water.

3.4 Skin Depth

An important parameter to understand electromagnetic propagation in a material is the skin depth δ_m, which is given by:

$$\delta_m = \frac{1}{\sqrt{\pi f \mu \sigma_m}}, \tag{3.6}$$

where f is the frequency and μ is the permeability of the material. The skin depth is given at which the electromagnetic field strength in the tissues falls to $1/e$ of its original value. When the frequency is low, the permittivity is relatively high and thus the conductivity is low, and the electromagnetic wave can propagate through the tissues without too much attenuation. At higher frequencies, the loss is increased, and hence the skin depth decreases, (see figure 3.3).

3.5 Tissues at a Single Frequency

To summarize the electrical properties relevant to this thesis, a table with several tissues evaluated at 3.5 GHz is given in table 3.1. However, the human body is layered with different tissues, depending on the anatomical location on the body. Hence, the layered structure of skin, fat, muscle, bone and target is complex and acts as a load to the used microwave antenna. Often, the thickness of each layer is not known or maybe a tissue layer is even infiltrated with fat.

Further, dielectric properties of tissues are not only frequency dependent, but also temperature dependent. Lazebnik *et al.* [Lazebnik et al., 2006] studied the frequency and

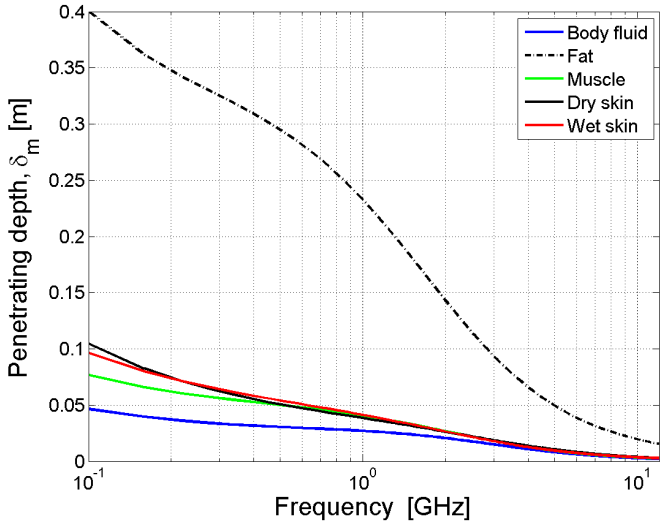

Figure 3.3: Skin depth versus frequency for some body materials [IFAC, 2011].

Table 3.1: Electrical properties of human body tissues at 3.5 GHz [IFAC, 2011].

Tissue	ε_r	σ_m [S/m]	δ_m [mm]
Body fluid	67.4	3.47	12.7
Blood	56.5	3.57	11.4
Muscle	51.4	2.56	15.0
Kidney	50.6	3.35	11.4
Wet skin	41.5	2.31	15.0
Mucous membrane	41.5	2.31	15.0
Dry skin	37.0	2.02	16.1
Bladder	17.5	0.99	22.6
Bone cancellous	17.4	1.20	18.8
Fat	5.2	0.16	77.9
Breast fat	5.0	0.22	54.0

temperature dependency of biological tissues, by using a single-pole Cole Cole model to fit the frequency dependency and a second-order polynomial to model the temperature variation. The paper also presents a table of previously published temperature-dependent dielectric properties, but the table has a lack of information on frequency and tissue specification. However, in their paper they reported a temperature coefficient in animal liver. The reported temperature coefficient $\frac{\Delta\sigma}{\sigma}$ [$\%^\circ$ C^{-1}] at 2.45 GHz for heating to be 0.20 with a standard deviation 0.33 and for cooling to be 0.008 with a standard deviation of 0.21. At the same frequency and tissue, the temperature coefficient $\frac{\Delta\varepsilon}{\varepsilon}$ [$\%^\circ$ C^{-1}] was for heating -0.17 with standard deviation of 0.30 and for cooling -0.09 with standard deviation of 0.06. This shows that the temperature coefficient is a parameter that in general has to be taken into account.

Furthermore, Ulaby *et al.* [Ulaby et al., 1986] has described a model in appendix E.2 in their book, on how to model the dielectric constant for water versus temperature. The high frequency limit $\varepsilon_\infty = 4.9$ and for a temperature T in °C, the relaxation time is:

$$\tau_r(T) = (1.1109 \times 10^{-10} - 3.824 \times 10^{-12}T + 6.938 \times 10^{-14}T^2 - 5.096 \times 10^{-16}T^3)/2\pi \quad (3.7)$$

and further, the low frequency limit is given by:

$$\epsilon_s(T) = 88.045 - 0.4147T + 6.295 \times 10^{-4}T^2 + 1.075 \times 10^{-5}T^3. \quad (3.8)$$

Then we can use eqs. (3.2a) and (3.2b) to find $\varepsilon(T)$. Temperature dependence on the dielectric constant in water is depicted in figure 3.4 for a fixed temperature range. Further, by using eq. (3.5) with eqs. (3.7) and (3.8) in eqs. (3.2a) and (3.2b), we can plot conductivity versus temperature, as seen in figure 3.5 for a fixed temperature range.

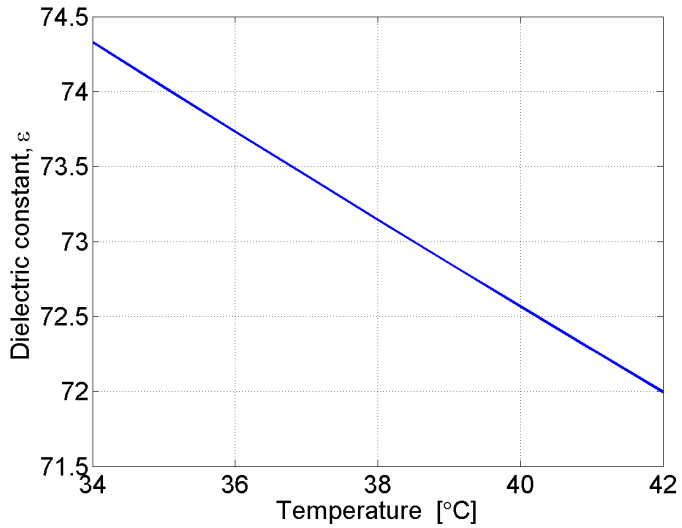

Figure 3.4: Dielectric constant versus temperature at 3.5 GHz for water.

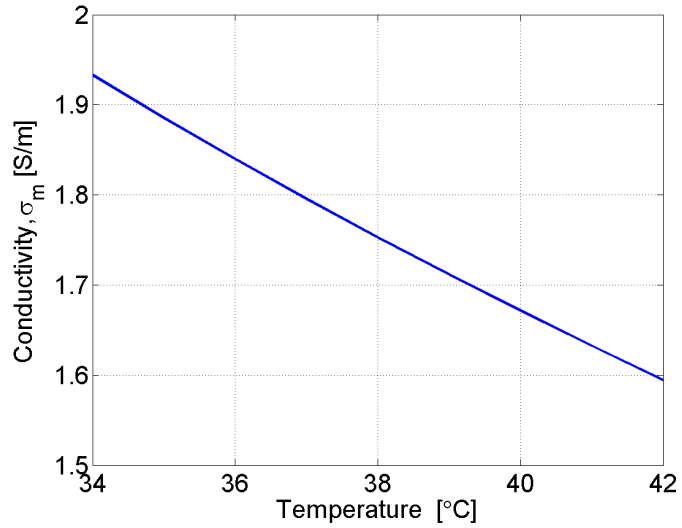

Figure 3.5: Conductivity versus temperature at 3.5 GHz for water.

Chapter 4

Radiometer Design and Realization

Design of a radiometer requires many, and at times, difficult choices and tradeoffs. The selection of frequency band must be deliberate and requires insight on how the penetration depth and antenna specific absorption rate (SAR) affect this choice. Another important factor is electromagnetic interference (EMI) and how the national frequency bands are distributed and used. However, when the frequency band once has been selected, the next step is to search for suitable components to be used in the front-end section of the radiometer. The internal noise produced by the radiometer affects the radiometer sensitivity (see section 2.2), and should therefore be as low as possible. As mentioned earlier, the temperature we want to measure is related to the thermal noise signal and its power density is extremely weak. To achieve sufficient power in the detector, there is a need of a wide integration frequency band and high amplification gain. Temperatures measured *in-vivo* at various parts of the human body with a core temperature of 37 °C (310 K), will give a power density $P_D = kT =$ 4.28 $\times 10^{-21}$ W/Hz or -173.69 dBm/Hz at the antenna input. By designing a front-end with a bandwidth of 500 MHz, for example, the power will increase to $P = kTB$= 2.14 $\times 10^{-12}$ W = -86.7 dBm after integration. This low power has to be further amplified for possible detection. A square law detector will typically require a level which is in the range -50 to -25 dBm. To obtain this power level requires an amplification in the front-end section of typically 50-60 dB. To achieve such amplification, a cascade of two or more amplifiers is needed at least for miniaturized drop-in components. This cascade can potentially cause instability problems (oscillation) by mismatch between each component.

The signal levels are illustrated at different blocks in figure 4.1. It is interesting to observe that a temperature difference of $\Delta T = 0.1$ K gives a $\Delta V_{out} = 0.13$ μV. Thus, we see the challenge of amplifying small DC values accurately affected by offset errors introduced by operation-amplifier (op-amp). Chopping the DC with switches is an excellent way to get around these problems [Enz et al., 1987, Bakker et al., 2000].

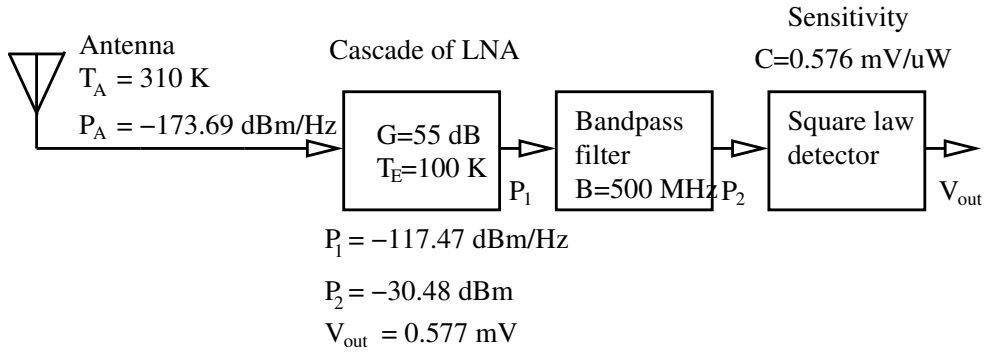

Figure 4.1: Signal levels at different blocks. The bandpass filter is assumed lossless.

4.1 Characterization of Radiometers

Before we describe the designs of radiometers in detail, we need some tools to test the radiometer performance. The gain and bandwidth of the radiometer can be measured with use of a network or a spectrum analyzer. The equivalent or system noise in the radiometer can be measured with a noise figure analyzer or indirectly by the Y-factor method [Pozar, 2004].

4.1.1 Radiometer Stability

A stable radiometer is mandatory in medical applications. The stability of a radiometer is depending on several factors including power supply stability, internal oscillations and temperature variations being the most important. Difficulties may arise from gain drifts of the front-end and back-end sections and also due to offset drift of the integrating electronics and the square-law detector.

Edwards *et al.* [Edwards and Sinsky, 1992] proposed an elegant method to determine the stability of a linear 2-port network. Other similar methods can be found in the literature [Pozar, 2004, Woods, 1976]. The Edward-Sinsky stability factor is defined as:

$$\mu = \frac{1 - |S_{11}|^2}{|S_{22} - S_{11}^* \cdot \Delta| + |S_{12} \cdot S_{21}|} > 1 \tag{4.1}$$

where S_{ij} and Δ are elements and the determinant of the scatter parameter matrix **S**, respectively. The system is unconditionally stable if $\mu > 1$.

4.1.2 Y-factor Method

The Y-Factor method is the basis of most noise figure measurements whether they are manual or automatically performed internally in a noise figure analyzer. Using a noise source, this method allows the determination of the internal noise in a device under test (DUT) and therefore the noise figure or equivalent noise temperature.

The method is implemented with the DUT connected to two different and known noise sources at different temperatures. Assume $T_1 > T_2$, and P_1, P_2 are the outputs from the noise sources 1 and 2, respectively. The equivalent noise temperature of the device under test is T_E. With this method we have two equations:

$$\hat{P}_1 = GkB(T_1 + T_E), \tag{4.2}$$

$$\hat{P}_2 = GkB(T_2 + T_E), \tag{4.3}$$

and define

$$\hat{Y} = \frac{\hat{P}_1}{\hat{P}_2} = \frac{T_1 + T_E}{T_2 + T_E}. \tag{4.4}$$

Here, $\hat{P}_1$ and $\hat{P}_2$ are measured to estimate $\hat{Y}$. We solve (4.4) with respect on T_E, that give us an estimate of the equivalent noise temperature in the device:

$$\hat{T}_E = \frac{T_1 - \hat{Y}T_2}{\hat{Y} - 1} \tag{4.5}$$

4.1.3 Allan Deviation

The commonly used standard deviation of a signal provides a measure of the signal statistical fluctuations. The weakness of the standard deviation is that it does not distinguish between random noise and other types of signal drift. On the other hand, the Allan deviation method has potential to differentiate between white noise, flicker noise, random-walk drift as well as systematic long term signal drift [Allan, 1987]. Land *et al.* [Land et al., 2007] used the Allan deviation to analyze the signal behavior of two different types of microwave radiometers. The Allan variance is a two-sample variance made by averaging the squared difference between two values of the measured temperature, over a sampling periods half of the measurement time. Hence, it is a made of a variance on measurement to measurement variation [Allan, 1987, Riley, 2008].

The Allan deviation seeks to quantify temporal measurement variations within a time series and is defined as [Barnes et al., 1971, Allan, 1987]:

$$\sigma_T(\tau_s) = \sqrt{\frac{\sum_{k=1}^{N-1}(T_{k+1} - T_k)^2}{2(N-1)}}, \tag{4.6}$$

where τ_s is the sampling period of N measurements of T_k for $k = 1 \ldots N$.

If different spectral noise components appear with separate spectral density power laws, then they can be described in a log-log plot of the Allan deviation versus the sampling period τ_s. Hence, different types of noise can be distinguished by the slope of the plot in various time regions. For microwave radiometry, the relevant types of signal variations are [Land et al., 2007]: a) Gaussian noise (slope of -0.5), b) Flicker noise (slope of 0), c) Random-walk noise (slope of 0.5), and d) long term steady drift (slope of 1).

An example plot of this behavior is given by Czerwinski *et al.* [Czerwinski et al., 2009], Land *et al.* [Land et al., 2007] and is also shown in paper 1 of this thesis (see section 6.1 [Klemetsen et al., 2011]).

4.2 Design

The choice of radiometer operation frequency is a challenge, since the penetration depth and lateral spatial resolution both are frequency dependent. An optimum frequency for microwave radiometry measurements of the human body is in the literature stated be around 3.2 GHz. This frequency allows reasonable penetrating depth and lateral spatial resolution [Campbell and Land, 1992, Land, 1987]. Another advantage with this frequency is less electromagnetic interference within this frequency band, compared to other frequency ranges that contain cellular phones and wireless networks. Once the frequency band is chosen, the next step is to find applicable microwave components that are surface mounted devices or SMD type. With SMD components, the physical size and cost can be reduced markedly of the system. However, the front-end microwave components has to produce a minimum of internal noise to produce optimal sensitivity, as described in section 2.2.1. The internal noise or equivalent noise temperature in a cascade is given by [Ulaby et al., 1981]:

$$T_E = T_{E1} + \frac{T_{E2}}{G_1} + \frac{T_{E3}}{G_1 G_2} + \cdots + \frac{T_{EN}}{G_1 G_2 \ldots G_{N-1}}, \tag{4.7}$$

where T_E is the total equivalent noise in the cascade and T_{Ei} and G_i for $i = 1, 2, 3, \ldots N$, is the internal noise and gain and/or loss respectively in each component.

A proper lay-out of the printed circuit board (PCB) of the front-end is important to avoid internal oscillations caused by parasitic effects and feedback through shared lines as DC supply and control lines. Even if the proposed design is simulated with commercial software such as CST Microwave Studio[1] and no such instability is revealed in the simulation, the physical design can have it. This recurring problem is common in microwave circuits and even more problematic in miniaturized designs.

4.2.1 Radiometer Realization

Two different designs were realized. A conventional Dicke radiometer (see figure 4.2) and a frontend with low noise amplifier (LNA) before the Dicke switch (see figure 4.3). An optional control circuit can be used to lock the switch in reference position and/or set the first LNA in a bypass mode, during a microwave heating sequence to protect the radiometer.

The frontend of the radiometer with the LNA before the switch is designed based on the results obtained in [Jacobsen and Klemetsen, 2008] and is paper 5 in the thesis (see section 6.5). A low noise amplifier before the Dicke switch for both the antenna and reference input, has a consequence of providing better sensitivity as the equivalent internal system noise is reduced. The used low noise amplifier is a Hittite HMC593LP3 with two modes; LNA and bypass. Typical noise figure with +5 V, 40 mA supply is 1.2 dB and

[1] http://www.cst.com/

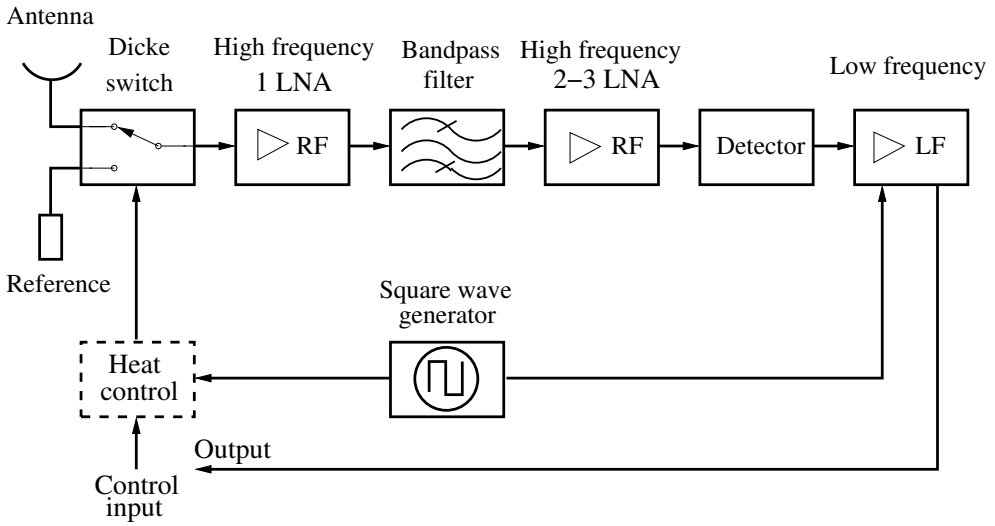

Figure 4.2: Block schematic frontend of the radiometer with an optional control of the switch, when used in a combination with microwave heating.

19 dB gain for a frequency range 3.3−3.8 GHz. The LNA has internal DC block capacitors on input and output. A Dicke switch is realized with a Mini−Circuit CSWA2-63DR+ switch, with insertion loss of typical 1.0 dB and of a single pole double throw (SPDT) type. The switch needs external DC block capacitors on all ports. A booster amplifier is a cascade of two Hittite HMC593LP3 LNA's followed by a combination of Mini−Circuit low pass filter LFCN-3400+ and high pass filter HFCN-3100+ that form the band pass filter. The output power of both designs was measured with an Agilent E4419B power meter containing an E4412A sensor. The Dicke switch controlling was conducted with use of a USB-3114 device from Measurement Computing[2] and LabVIEW. The results of these designs are described in detail in the included paper 1 (see section 6.1) [Klemetsen et al., 2011]. Further, the same design with use of Hittite detector HMC602LP4 is illustrated for the front-end in figure 4.4. The low frequency part is shown in figure 4.5 with the PCB layout in figure 4.6 for the schematic diagram.

Another radiometer was designed following the principle described by D.V. Land [Land, 2001]. The principle uses a circulator to avoid mismatch from the used antenna and hence possible instability in the following frontend (see figure 4.7). This design mainly applies the same components as described above, but is further improved with use of a circulator of type 3CDMG35-4 from Dorado International as well as a more sensitive detector of type HMC602LP4 from Hittite. Hittite HMC602LP4 logarithmic detector has excellent stability with temperature and a superior sensitivity of -26 mV/dB. The LF (low frequency) circuit (designed by Senior Engineer Karl Magnus Fossan at Department of Physics, University of Tromsø) is a combination of an amplifier and a synchronous demodulator. Here, the amplification is obtained with low noise opera-

[2]www.mccdaq.com

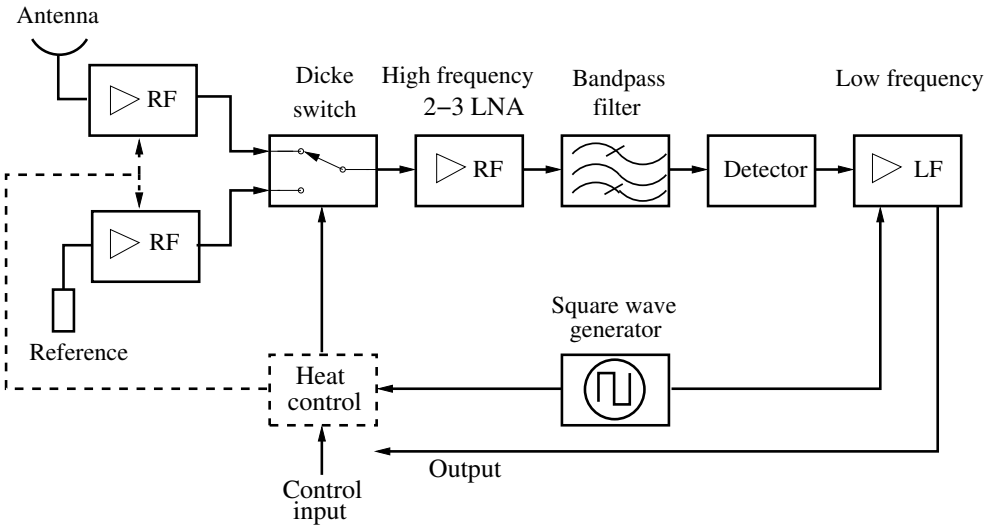

Figure 4.3: Block schematic frontend of the radiometer with an optional control of the switch and the first, low noise amplifier (LNA), when used in a combination with microwave heating.

tion amplifiers LT1028 and the synchronous demodulator is a sampling and hold circuit to get the difference between the antenna and reference signal (LTC1043 - dual precision instrumentation switched-capacitor building block), both from Linear Technology. The synchronous demodulator is described in detail in figure 4.8.

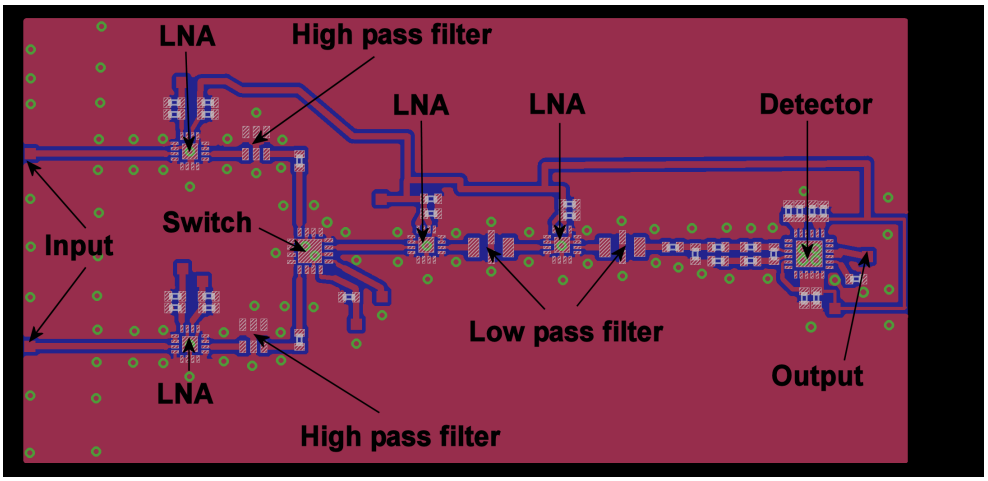

Figure 4.4: PCB layout for design with LNA in front and Hittite detector HMC602LP4.

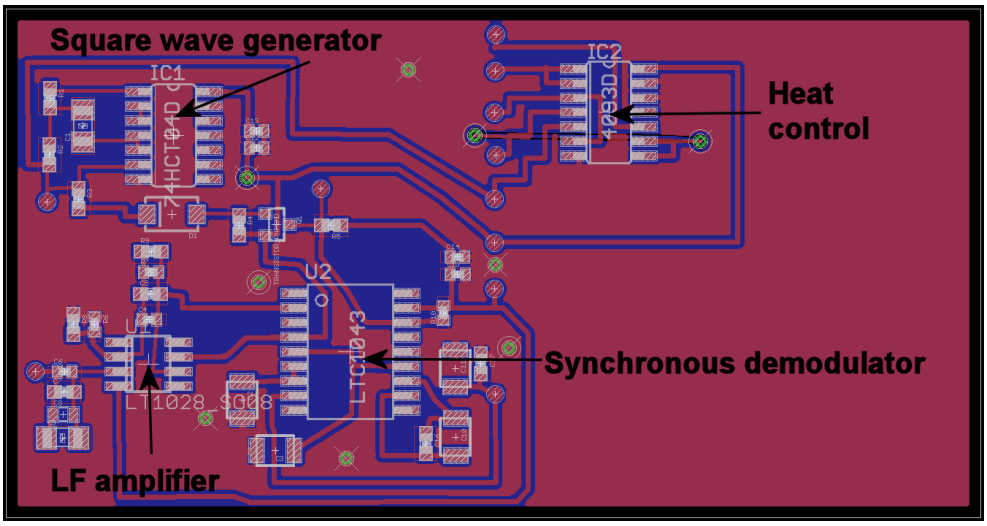

Figure 4.5: PCB layout for the heat control, LF amplifier and synchronous demodulator design.

4.2.2 Prototype of a Complete Miniaturized Radiometer

The main idea was to build a complete miniaturized radiometer that was directly controlled by a PC via USB connection. One requirements was to have known cold and

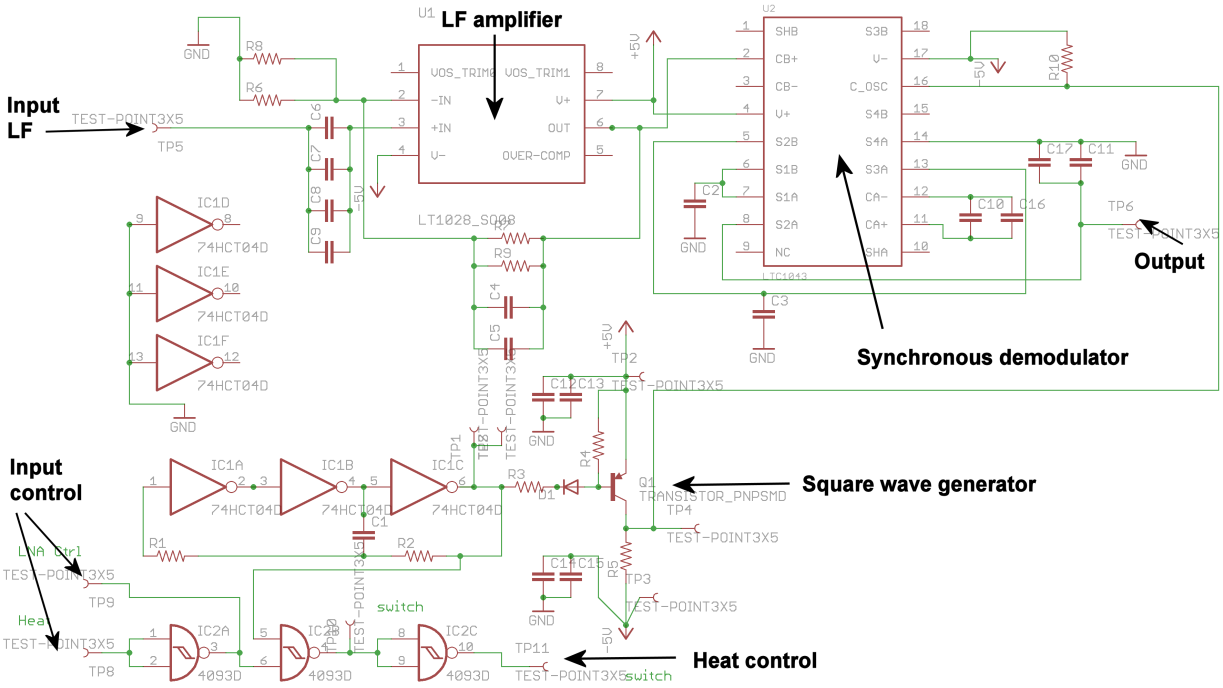

Figure 4.6: Schematic diagram for the heat control, LF amplifier and synchronous demodulator design.

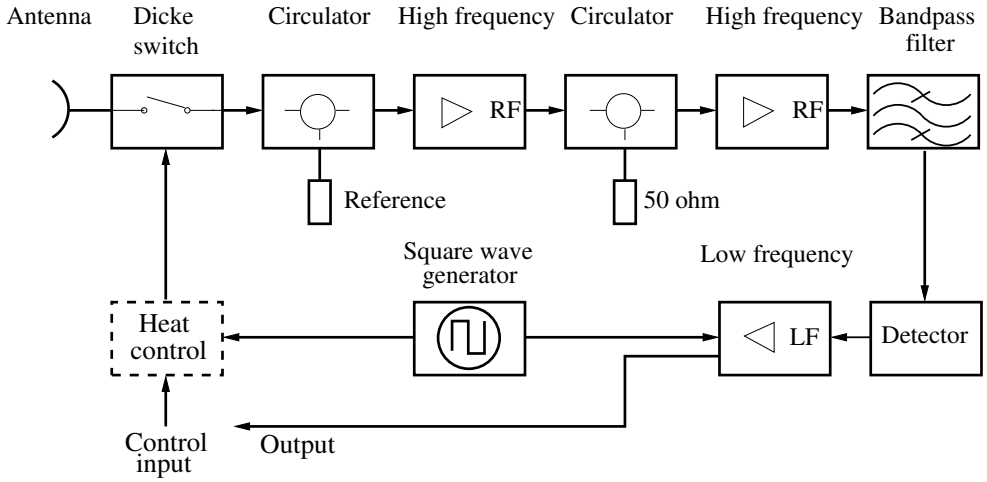

Figure 4.7: Block schematic frontend of the radiometer with use of a circulator and an optional control of the switch, when used in a combination of microwave heating.

a hot references for self calibration of the radiometer and an additional conventional known reference at the input connection. To perform the calibration, a rat-race [Pozar, 2004] described in details by Mo *et al.* [Mo et al., 2007] was scaled, designed and implemented to fit our frequency band. The calibration part and the radiometer front part was connected to each input ports and the output was the sum port with the difference port terminated to 50 Ω. The output from the rat-race then goes to the booster amplifier, band pass filter, detector circuits and low frequency amplifier. An analog-digital converter (ADC) was realized with use of a National Instrument USB-6009 data acquisition circuit. The USB-6009 data acquisition (DAQ) was used to control the Dicke switch in both front part and calibration part, measuring three different temperatures, warming the hot reference and as ADC from the low frequency amplifier output. The power supply to all circuits was taken from the USB connection. To ensure a more stable voltage at the internal USB +5 V, an additional +5 V power supply was used. The complete ra-

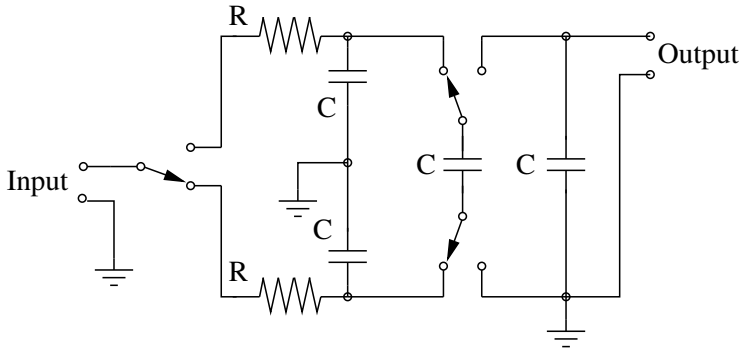

Figure 4.8: Detailed schematic diagram of the synchronous demodulator, with use of switched-capacitor building blocks.

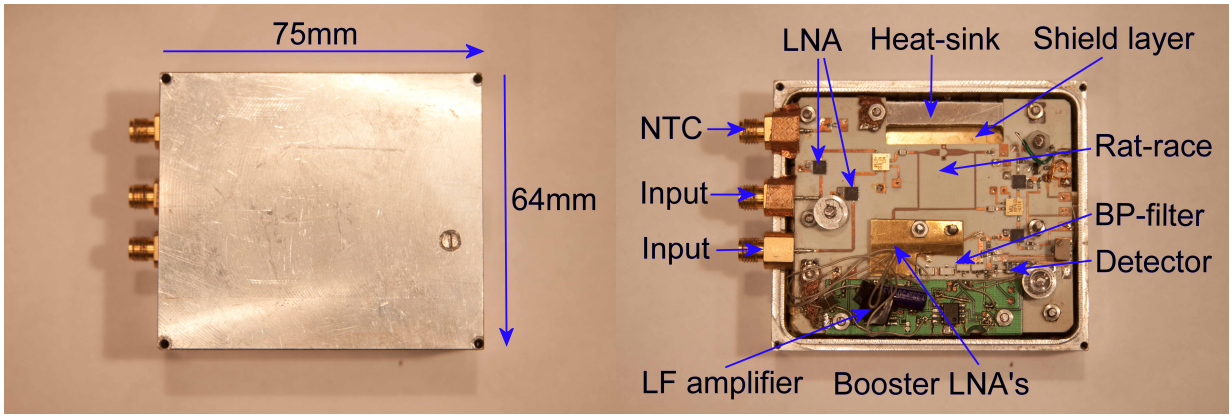

(a) Miniaturized Radiometer (b) With open top cover

Figure 4.9: Miniaturized radiometer with dimensions and details of the circuits.

diometer was put in a metal box H×W×D dimensions of 35×75×64 mm^3 respectively (see figures 4.9a and 4.10).

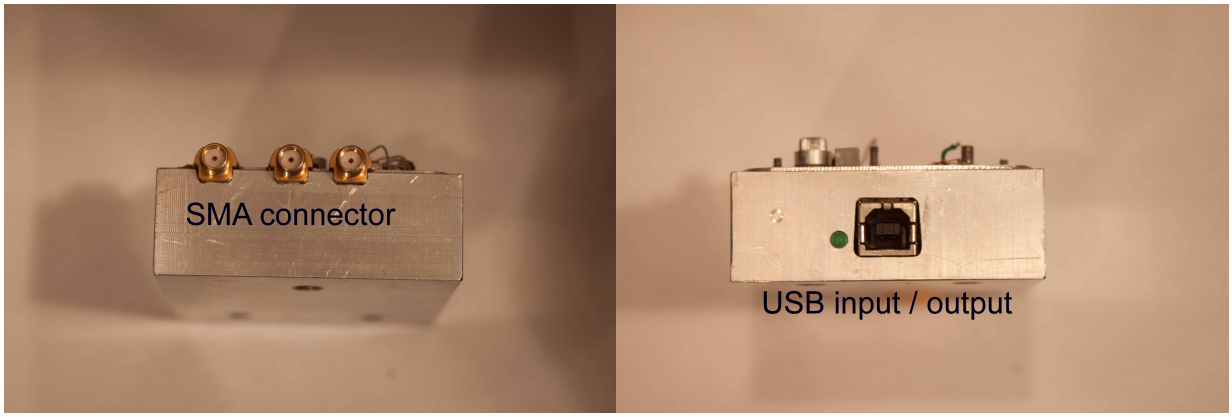

(a) SMA connectors to the antenna (b) USB input/output with internal powerline.

Figure 4.10: Radiometer with open top cover and the input/output connections.

The front part of the radiometer is designed as described above, with LNA, before the Dicke switch and with mainly the same components. Surface mount microwave Schottky detector diode HSMS-2865 from Avago Technologies[3] was used with external bias for the detector. Linear Technology[4] LT1028 - ultra low noise precision high speed operation amplifier was used in the low frequency amplifier, mounted on a typical FR4 printed circuit board. The high frequency layout was designed and simulated with use

[3]www.avagotech.com
[4]www.linear.com

of CST Microwave Studio[5] to complete the complex rat-race implementation. The high frequency parts are mounted on a printed circuit board (PCB) RO4350B, (Rogers Corp., USA) of 0.254 mm thickness. The PCB is further mechanically stabilized with use of a metal plate that also acts as a heatsink. A shielded layer is placed in between the DAQ and the high and low frequency part to avoid interference (see figure 4.9b). The connection to the DAQ is going via solder-in filters in the shielded layer.

The complete radiometer system with a connected shielded elliptical antenna is illustrated in figure 4.11. The three coaxial cables going from the radiometer are the antenna input, reference input and reference temperature measurement input, respectively. The reference is a surface mount 50 Ω resistor and the temperature sensor for the reference is of a negative temperature coefficient (NTC) type, also surface mount.

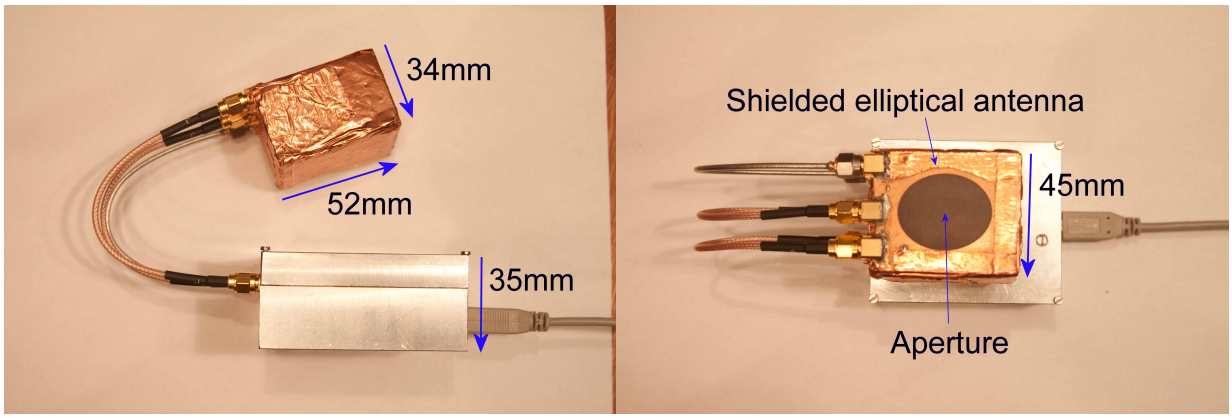

(a) Side view (b) Top view

Figure 4.11: The radiometer with connected antenna.

[5] www.cst.com

Chapter 5

Antennas in Medical Applications

Antennas are one of the most critical components in EM radio communication systems [Balanis, 1992, Balanis, 2005]. An antenna should be able to radiate effectively, often in a certain direction, and generally be of smallest possible physical size. There is a need for antennas in systems ranging in size from small cell phones to huge radar systems. Antennas are cheap in RFID systems and costly in satellite systems. Furthermore, antennas can be made as simple wire antennas to complex high-tech phased arrays.

However, the antenna to be used must be approximately designed for the desired operation frequency, bandwidth, beam direction and the medium that the antenna will radiate into. It is common to use commercial electromagnetic simulation software in the design of various antennas. An antenna built from a specific design is then tested to see if it provides the qualities that one would expect. Receiving antennas are usually tested in active mode rather than in passive mode, since they in general are reciprocal [Carr, 1989].

Furthermore, antennas used in medicine, may be more sophisticated depending on the application. Antennas to be used on or implemented inside the human body require totally different designs than those used in air, since the dielectric properties are different and most often includes heterogeneous loads.

Generally, the body is built up in layers of different tissue types which have different dielectric properties. An antenna used non-invasively on the human body has to be matched to the anatomical structure of the body and must also provide good contact with the body so that the antenna characteristics are not degraded. If the antenna is poorly fitted to the human body and/or the patient is moving, the power transfer from or till the antenna will be affected.

Another important factor is shielding of the antenna. An active antenna should be shielded in such a way that it does not radiate unnecessary power to the surroundings, and such that it does not interfere with other equipment. A passive antenna or a receiver antenna must also be shielded, so that unwanted electromagnetic interference (EMI) does not disturb the receiver.

5.1 Types of Antenna for Medical Applications

Many medical antennas have been designed and realized over the years. Some are patented, some are successful while others have never had the spread that was intended. Antenna technology for medical applications is a major research field, ranging from simple monopole antennas to more advanced phased array antennas. To review all antenna types is beyond the scope of this thesis. We therefore limit obviously to only include antenna designs that we regard as most important for the medical observation technique that is under study (microwave radiometry).

In microwave sensing, there are several types of antennas that can be used, e.g. monopole, dipole, coil, waveguide, horn and printed circuit board (PCB) antennas. Printed circuit board antenna can be of different types e.g. spirals, patch and slots antennas. Depending on the application, some of the antennas have to be fitted directly on the human body, and can be made small due to the dielectric scaling of the body compared to air. Printed circuit board (PCB) antennas have the advantage of a simple production process and can be fitted to the body directly. The main challenges in microwave antenna design for medical application are effective coupling and the penetration ability into heterogeneous lossy body tissues since the antenna is operating in the antenna near field. In microwave radiometry, printed circuits board antennas have to be properly shielded to avoid EMI. Hence, shielding can make them bulky compared to the low-profile PCB antennas [Stauffer and Maccarini, 2011].

Antennas can be used for communication with implants that contain an antenna. On-body communication with an implanted medical electronic device, so called body area network (BAN), is also of interest in military, multimedia and sport applications [Chahat et al., 2011]. Antennas for wireless body area network (WBAN) can have different designs, but small size and an ultra wide frequency band realization are preferable, due to their high transmission rate needed for many applications. BAN and WBAN have also interest in telemedicine where there is a need of wearable health monitoring systems, that can be used for instance in activity-, breathing-, electrocardiogram- and blood pressure-monitoring [Jovanov et al., 2005].

Waveguide antennas can radiate via broad wall slots or via open-ended waveguides [Rengarajan, 1989]. To match an open ended waveguide antenna to the human body, a dielectric filled waveguide can be used [Carr, 1989]. Thus, medical waveguide antennas are used in hyperthermia cancer therapy [Boag and Leviatan, 1993], in medical radiometry system [Cheever and Foster, 1992] and in UWB radar detection of breast tumors [Fear et al., 2002a]. Horn antenna is an opened up waveguide, and can be flared out in the E-plane, H-plane or in both planes, often called a pyramidal horn. The horn antenna is typically fed by a section of a waveguide. The waveguide itself is fed with a short dipole [Bevelacqua, 2011]. The dielectric horn antenna is an antenna filled with a dielectric material to obtain better matching to a layered phantom or human body,

when used in a UWB breast imaging application [Amineh et al., 2009]. The Lucite-Cone applicator is a modified water filled horn-antenna, with a replaced diverging E-field wall, that is parallel to the E-field. A second modification is the use of a PVC cone positioned in the plane of the aperture [Van-Rhoon et al., 1998]. The Lucite-Cone applicator is characterized by a large effective field size and is used in microwave hyperthermia treatment [Van-Rhoon et al., 1998, Rietveld et al., 1999, Samaras et al., 2000]. This applicator can also be extended to a larger field on the body by an array configuration.

The dual concentric conductor (DCC) antenna is a printed circuit board antenna that is used in hyperthermia treatment and recently as a heating antenna for warming the bladder prior to VUR detection [Stauffer et al., 1998, Snow et al., 2011a]. The DCC antenna can also be in an array applicator (conformal PCB arrays) for large area used in chest wall disease [Stauffer et al., 2010]. There is also been conducted research on a combination antenna, that can be used for both hyperthermia and microwave radiometry to monitor the heating process through temperature reading [Jacobsen et al., 2000]. Hyperthermia is also used in magnetic resonance (MR) thermal imaging that uses coils and dipole phased arrays for heating extremity tumors [Wyatt, 2010].

Current research on antenna involves metamaterials, materials that have engineered dielectric and magnetic constants, which can be simultaneously negative. Due to the engineered material, it has properties that may not be found in nature. Metamaterials have interesting properties like a negative index of refraction [Bevelacqua, 2011]. To effectively manipulate an electromagnetic wave of any kind, the metamaterial slab used has to be smaller than the wavelength. Hence, it could be used for microwaves, since the wavelength is in the centimeter range. Recently introduced medical metamaterial antennas have the ability to focus inside biological tissues due to use of a metamaterial lens [Stauffer and Maccarini, 2011, Gong and Wang, 2009].

Recent trends in antenna development go towards smaller antennas, which are better adapted to different anatomical locations. Microstrip antennas is preferred since they are easy to make and inexpensive to produce.

5.2 Elliptical Antenna

Many antenna designs have been proposed for microwave radiometry. To design and construct an antenna is a research field by its own as mentioned above, and the best way to find a suitable antenna is to look in the literature. In my research group, several designs have been under investigation [Jacobsen et al., 2005, Jacobsen and Stauffer, 2001, Jacobsen et al., 2000, Stauffer et al., 1998, Stauffer and Maccarini, 2011]. The choice of antenna is depending on the used frequency band, physical size and the penetrating ability in the human body. The selected antenna in this thesis is a modified version of a low-profile, single-ended, planar, elliptical antenna [Powell and Chandrakasan, 2004, Jacobsen and Birkelund, 2010, Brelum, 2010]. The elliptical antenna has a microstrip feed, elliptically shaped patch on the back side and a larger elliptically shaped aperture on the front side for mounting onto the human body. Due to electro-magnetic

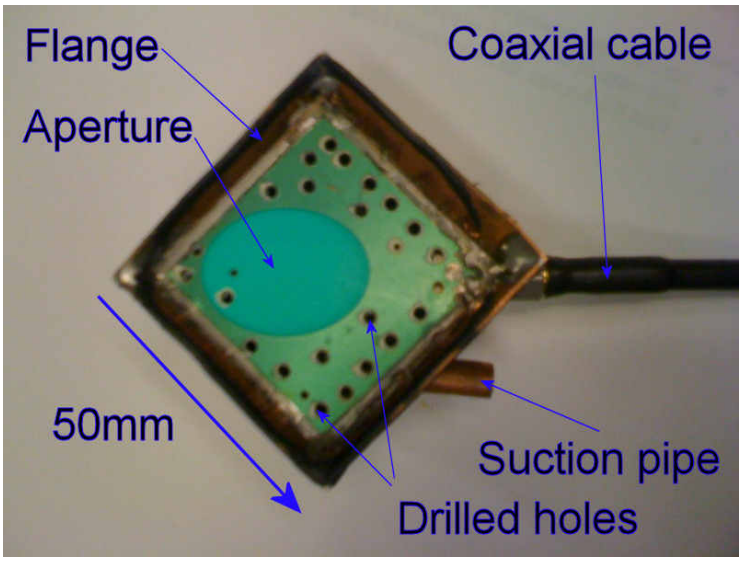

Figure 5.1: The proposed suction antenna with drilled holes in the antenna front surface and vacuum pipe connection.

interference (EMI) that can disturb the extremely low thermal signal from the body, Arunachalam *et al.* [Arunachalam et al., 2010, Arunachalam et al., 2011] proposed to shield the printed circuit board log spiral antenna with a shield cup on the back of the antenna to avoid EMI. To shield the elliptical antenna, Birkelund *et al.* [Birkelund et al., 2010] used rectangular box shielding with use of copper tape soldered together. A simulation and measurement of the specific absorption rate (SAR) of this antenna on phantoms is presented in paper 4 (see section 6.4) [Birkelund et al., 2011].

The elliptical antenna is further modified with use of rectangular box shielding of copper plate and a flange around the front to improve the shielding when loaded on the human body. The flange elliptical antenna is used in paper 2 and 3 of this thesis (see sections 6.2 and 6.3).

5.3 Elliptical Antenna with Suction

An elliptical antenna with suction was proposed after an animal *in vivo* experiment where we used elastic bands to hold an antenna steady in a given position. The use of elastic band posed a question: Is the antenna in the correct position and properly mounted on the skin during the whole experiment? The answer was not given directly, because the antenna was mounted underneath the elastic band and not so easy to observe during the measurements. The next question was: Can the antenna be mounted more securely, without use of elastic bands?

The main idea of the suction antenna is to use negative pressure to mount the antenna onto the human body. This idea is the main topic in paper 3 of this thesis (see

section 6.3) [Klemetsen and Jacobsen, 2011].

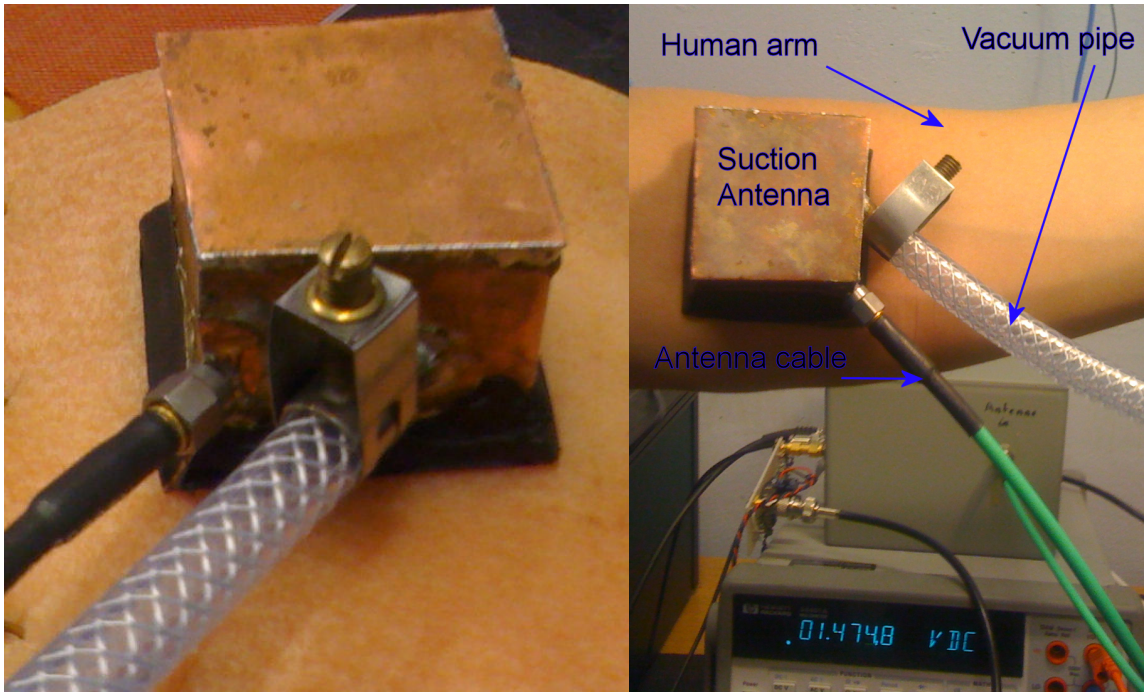

(a) *In-vitro* on animal skin (b) *In-vivo* on human arm

Figure 5.2: Pre-test of the negative pressure antenna mounted *in vitro* and *in vivo*.

The suction antenna is made from a Rogers RO-4350B substrate of thickness 1.524 mm, dielectric constant ε_r = 3.66 and a loss tangent tanδ=0.0037. The antenna has frontal dimensions of 40×40 mm^2 and was electrically shielded by a cavity backing of 32 mm height to avoid electromagnetic interference. The back-cavity was made of 0.7 mm copper plates soldered together. A flange around the antenna and cavity was made to improve shielding for reducing EMI. Including the flange, the total outer front dimensions become 50×50 mm^2. The holes in the antenna front surface were drilled randomly, but care was taken to avoid the microstrip, elliptical patch on the back and the coaxial connector on the printed circuit board. An adjustable vacuum pump with a pressure meter is used to regulate the negative pressure on the antenna. The used antenna is illustrated in figure 5.1.

A pre-test of the antenna mounted *in vitro* on an animal skin and *in vivo* on a human arm is demonstrated in figure 5.2. Notice that the antenna in figure 5.2b is maintained in a vertical position on the arm entirely by use of suction.

Chapter 7

Conclusions and Future Work

This chapter contains conclusions, a discussion of pertinent challenges we have faced as well as suggestions for possible improvement in future versions of this technology. Microwave radiometry was proposed as a medical modality way back in the seventies. With commercially more compact microwave components available today, a modern microwave radiometer can be made cheap and small in size. Due to the reduction in power and size of electronic components, a more stable radiometer can also be developed. Gunnarsson *et al.* [Gunnarsson et al., 2008] reported a single chip radiometer operated at 53 GHz, so this is a plausible direction of designing future radiometers. Our radiometers are designed for medical applications, and there is still a need for more research and development in this field, before this technology can be commercialized.

7.1 Conclusions

In this thesis, it has been shown that it is possible to design, simulate and built a small sized microwave radiometer for use on realistic human phantoms. Even more important, experiments show that the radiometer can be used *in-vivo* to mimic realistic temperature measurements within the human body. Suction on a microwave PCB antenna has shown improved radiometric performance. The simple and yet elegant solution for coupling of the antenna with use of negative pressure, and the interpretability of the results, are taken as proofs of this statement.

7.1.1 Active Antennas

An active antenna in microwave radiometry was tested out in paper 1 and 5 (see sections 6.1 and 6.5) and the results show significantly better sensitivity for the radiometer compared to conventional variants. Further, the experiment in paper 5 was conducted with use of a monopole antenna. The used monopole antenna is not suitable for use on humans, because it was made of a rigid stripped coaxial cable, and coupling to the human body is not satisfactory.

7.1.2 Compact Radiometer Designs

The radiometer designs reported in chapter 4 are not presented in chronological order. The first radiometer designed was the miniaturized radiometer (see section 4.2.2). The intension of this design was miniaturization, but it turned out later that there were many factors that were not implementable in small scale. The main shortcomings in this early design were:

- **Dicke switch:** The Mini-Circuit CSWA2-63DR+ switch used in the realization process of the radiometers has different insertion losses for different switch positions. Typically, a difference between each position is about 0.1 dB at 3.5 GHz. This results in a temperature difference of about 7.2°C. This difference gives an error in the self-calibration of the miniaturized radiometer, since the difference varies with frequency and has to be compensated for. However, this problem does not affect radiometer designs using an external calibration process.
- **Realized rat-race:** The realized rat-race has a difference in the transmission between each input port. When used in sum configuration, this gives an error in the self-calibration process. An improved implementation of the rat-race where optimizing of dimensions of the rat-race can solve this problem.
- **Hot reference:** Warming the hot reference (in the calibration circuit) tends to give a temperature gradient on the printed circuit board that again affects the gain in the nearest LNAs and also disturbs the operation point of the used detector diode. This excess heat leads to saturation in the LF amplifier, and temperature drift in the cold temperature reference in the radiometer.
- **LabVIEW and DAQ:** The combination of LabVIEW and the DAQ USB 6009 is not fast enough to perform the Dicke switching, digital to analog converter (DAC) and analog to digital converter (ADC) operations in parallel, during operation of the prototype miniaturized radiometer.
- **USB connector:** The USB connection to the miniaturized radiometer can in some situations give instability problems in the internal drive voltage (+5V). The consequence is that the operation point of the complete radiometer circuit becomes different than preset and hence the absolute temperature measurements are not longer valid with the original calibration of the system.

7.1.3 Modular Second Generation Design

To continue the project, it was necessary to divide the radiometer into several modules, where each of the parts had to be tested separately. This resulted in the modular design described in section 4.2.1, with only the front-end and use of a commercial power detector from Agilent. This design was tested on realistic phantoms during heating and is described in paper 1 (see section 6.1). This design was further developed with use of a

surface mount detector from Hittite and a circulator from Dorado International. A new low frequency amplifier and a demodulator were also implemented. The results with use of this radiometer design are presented in paper 2 and 3 of this thesis. A printed circuit board layout with the front-end, the Hittite detector and the low frequency part was then developed but, the last design is not built. We point out that to gather all the threads and finish the construction of the final design is relatively straight forward, since all emerging problems are resolved, but not yet implemented.

7.1.4 Medical Applications

A radiometer with satisfactory specifications must be connected to a suitable antenna. A microwave radiometer must demonstrate realistic measurements values, relevant for medical applications. Measurements on phantoms are valuable, but *in-vivo* measurements in humans are of greater value. The problem is to find appropriate ways to do this, and at the same time be in compliance with ethical rules. One example of realistic measurement for the heating of a pediatric bladder is presented in paper 2 of this thesis (see section 6.2). Here, the use of a balloon inside the human mouth mimics the anatomical layers of a pediatric bladder. The flexible setup allows for both convective heat transfer using a closed loop liquid system and extensive use of fiber optic temperature probes to verify the radiometric temperature measurements.

The presented microwave radiometer and the suction antenna can also be used in other medical applications. Breast cancer detection may be the medical application of greatest potential and interest.

7.1.5 Medical Suction Antenna

The idea to use suction on an antenna to maintain the applicator in a given position during microwave radiometry, is novel and the results of these *in-vivo* experiments on a human body are presented in paper 3 of this thesis. The suction principle can be used for different antennas in different medical applications, including UWB radar applications, during hyperthermia and for other measurement scenarios when you need an antenna mounted directly onto the human body.

7.2 Future Work

The modular second generation radiometer in combination with the suction antenna shows excellent radiometric performance as documented by the papers of this thesis. Below is a summation of furher development that can be done with the instrumentation.

- **Development of a third generation radiometer:** Dedicated microcontroller devices can operate via USB and is one of the most important issues in future improvement of the radiometer system, since USB is the most common communication port in

a modern computer. A microcontroller can easily operate the Dicke switch and other switches with user-controlled clock speed. Even more important, it can also perform ADC and DAC operations.

The self-calibration issue of the radiometer has to be solved. The hot reference in the calibration sequence has to be thermally insulated to avoid thermal gradients on the PCB and hence prevent shift in the operation point of internal circuits. Self-calibration provides absolute temperature measurements, without external calibration of the system.

A radiometer with an LNA placed before the Dicke switch; that is with the LNAs, reference and switch implemented on the antenna PCB, can further improve the sensitivity. All loss/attenuation in coaxial cables contributes to the system equivalent noise in the complete system. Loss/attenuation occurring *after* a moderate gain amplifier, the whole system noise decreases and hence better sensitivity is obtained. A stacked configuration of antenna, thermal and EMI shielded layer, the HF frontend layer and then the LF and microcontroller layer, is a solution that should be evaluated in future work. Stacking all layers gives a small physical size of the complete system. Heatpipes can also be used to carry heat away. This solution is commonly used in e.g. laptops.

- **Development of a second generation suction antenna:** The positioning and diameters of the holes in the suction antenna aperture and flange have to be optimized to obtain maximum coupling to the body with lowest possible suction pressure. Irritation of human skin can be reduced by using less suction. The first generation suction antenna has a frontal square form. Corners of the square tend to leak air. A circular or elliptical frontal shape is preferable to improve coupling to different challenging antomical parts of the human body. A rubber outline of the flange can further improve suction performance and hence reduce the negative pressure needed to obtain adequate coupling to the body surface.

Bibliography

[Mob, 2011] *Mobile and accessible ultrasound imaging*. November 2011. Http://www.mobisante.com/.

[AHIP, 2008] AHIP. *Ensuring quality through appropriate use of diagnostic imaging*. http://www.ahip.org/content/default.aspx?docid=24057, July 2008. Americas Health Insurance Plans.

[Allan, 1987] D. W. Allan. *Should classical variance be used as a basic measure in standards metrology. IEEE Trans. Instrum. Measurements*, **36**(2): 646 –654, 1987.

[Amineh et al., 2009] R. K. Amineh, A. Trehan and N. K. Nikolova. *Tem horn antenna for ultra-wide band microwave breast imaging. Progress In Electromagnetics Research B*, **13**: 59–74, 2009.

[Arunachalam et al., 2008] K. Arunachalam, P. R. Stauffer, P. F. Maccarini, S. Jacobsen and F. Sterzer. *Characterization of a digital microwave radiometry system for noninvasive thermometry using a temperature-controlled homogeneous test load. Physics in Medicine and Biology*, **53**(14): 3883 3901, 2008.

[Arunachalam et al., 2010] K. Arunachalam, P. F. Maccarini, V. De-Luca, F. Bardati, B. W. Snow and P. R. Stauffer. *Modeling the detectability of vesicoureteral reflux using microwave radiometry. Physics in Medicine and Biology*, **55**(18): 5417–5435, 2010.

[Arunachalam et al., 2011] K. Arunachalam, P. Maccarini, V. De Luca, P. Tognolatti, F. Bardati, B. Snow and P. Stauffer. *Detection of vesicoureteral reflux using microwave radiometry - system characterization with tissue phantoms. Biomedical Engineering, IEEE Transactions on*, **58**(6): 1629 –1636, june 2011.

[Averkiou et al., 1997] M. Averkiou, D. Roundhill and J. Powers. *A new imaging technique based on the nonlinear properties of tissues*. IEEE Ultrasonics Symp., IEEE Ultrasonics Symp., 1997.

[Bakker et al., 2000] A. Bakker, K. Thiele and J. Huijsing. *A CMOS nested-chopper instrumentation amplifier with 100-nv offset. Solid-State Circuits, IEEE Journal of*, **35**(12): 1877 –1883, dec 2000.

[Balanis, 1992] C. Balanis. *Antenna theory: a review*. *Proceedings of the IEEE*, **80**(1): 7 –23, jan 1992.

[Balanis, 2005] C. A. Balanis. *Antenna theory*. Wiley Interscience, third edition, 2005.

[Ballew, 2006] L. R. Ballew. *A microwave radiometer system for use in biomedical applications*. Master's thesis, Baylor University, 2006. Http://hdl.handle.net/2104/4956.

[Barnes et al., 1971] J. A. Barnes, A. R. Chi, L. S. Cutler, D. J. Healey, D. B. Leeson, T. E. McGunical, J. A. Mullen, W. L. Smith, R. L. Sydnor, R. F. C. Vessot and G. M. R. Winkler. *Characterization of frequency stability*. *IEEE Trans. Instrum. Measurements*, **IM-20**(2): 105 –120, May 1971.

[Barrett and Meyers, 1975] A. H. Barrett and P. C. Meyers. *Subcutaneous temperatures: A method of noninvasive sensing*. *Science*, **190**(4215): 669–671, 1975.

[Bevelacqua, 2011] P. J. Bevelacqua. *The online source for understanding antennas*. http://www.antenna-theory.com/, October 2011.

[Birkelund et al., 2010] Y. Birkelund, Ø. Klemetsen, K. Arunachalam, V. De-Luca, P. F. Maccarini, S. Jacobsen and P. R. Stauffer. *Radiometric temperature monitoring of microwave hyperthermia*. Society For Thermal Medicine 2010 Annual Meeting, Clearwater Beach, FL,USA, April 2010.

[Birkelund et al., 2011] Y. Birkelund, Ø. Klemetsen, S. Jacobsen, K. Arunachalam, P. Maccarini and P. Stauffer. *Vesicoureteral reflux in children: A phantom study of microwave heating and radiometric thermometry of pediatric bladder*. *Biomedical Engineering, IEEE Transactions on*, **58**(11): 3269 –3278, nov. 2011.

[Blute and Lewis, 1991] M. L. Blute and R. W. Lewis. *Local microwave hyperthermia as a treatment alternative for benign prostatic hyperplasia*. *Journal of Andrology*, **12(6)**: 429–434, 1991.

[Boag and Leviatan, 1993] A. Boag and Y. Leviatan. *Analysis and optimization of waveguide multiapplicator hyperthermia systems*. *Biomedical Engineering, IEEE Transactions on*, **40**(9): 946 –952, sept. 1993.

[Brelum, 2010] S. H. Brelum. *Ultrawideband (UWB) imaging of breast tissue: A numerical study of planar elliptical antennas applied to ultrawideband (UWB) imaging of breast tissue*. LAP Lambert Academic Publishing, 2010.

[Broens et al., 2007] T. H. F. Broens, R. M. H. A. Huis in't Veld, M. M. R. Vollenbroek-Hutten, H. J. Hermens, A. T. van Halteren and L. J. M. Nieuwenhuis. *Determinants of successful telemedicine implementations: a literature study*. *J Telemed Telecare*, **13**(6): 303–309, 2007.

[Bryan et al., 2000] S. Bryan, M. Buxton and E. Brenna. *Estimating the impact of a diffuse technology on the running costs of a hospital*. *International Journal of Technology Assessment in Health Care*, **16**(03): 787–798, 2000.

[Bushberg et al., 2002] J. T. Bushberg, J. A. Seibert, E. M. L. Jr. and J. M. Boone. *The essential physics of medical imaging*. Lippincott Williams & Wilkins, second edition, 2002.

[Campbell and Land, 1992] A. M. Campbell and D. Land. *Dielectric properties of female human breast tissue measured in vitro at 3.2 GHz*. *Phys. Med. Biol*, **37**: 193–210, 1992.

[Carr, 1989] K. L. Carr. *Microwave Radiometry: Its Importance to the Detection of Cancer*. *IEEE Trans. Microwave Theory and Tech.*, **37**(12): 1862–1869, December 1989.

[Chahat et al., 2011] N. Chahat, M. Zhadobov, R. Sauleau and K. Ito. *A compact UWB antenna for on-body applications*. *Antennas and Propagation, IEEE Transactions on*, **59**(4): 1123 –1131, april 2011.

[Chang et al., 2008] T.-C. Chang, Y.-L. Hsiao and S.-L. Liao. *Application of digital infrared thermal imaging in determining inflammatory state and follow-up effect of methylprednisolone pulse therapy in patients with graves ophthalmopathy*. *Graefes Archive for Clinical and Experimental Ophthalmology*, **246**: 45–49, 2008. 10.1007/s00417-007-0643-0.

[Cheever and Foster, 1992] E. Cheever and K. Foster. *Microwave radiometry in living tissue: what does it measure?*. *Biomedical Engineering, IEEE Transactions on*, **39**(6): 563 –568, june 1992.

[Christopher, 1998] T. Christopher. *Experimental investigation of finite amplitude distortion-based, second harmonic pulse echo ultrasonic imaging*. *Ultrasonics, Ferroelectrics and Frequency Control, IEEE Transactions on*, **45**(1): 158 –162, jan 1998.

[Czerwinski et al., 2009] F. Czerwinski, A. C. Richardson and L. B. Oddershede. *Quantifying noise in optical tweezers by allan variance*. *Optics Express*, **17 Issue 15**: 13255–13269, 2009.

[Diakides and Bronzino, 2008] N. A. Diakides and J. D. Bronzino. *Medical Infrared Imaging*. CRC Press. Taylor & Francis Group, 2008.

[Dubois et al., 1996] L. Dubois, J. Sozanski, S. Tessier, J. Camart, J. Fabre, J. Pribetich and M. Chive. *Temperature Control and Thermal Dosimetry by Microwave Radiometry in Hyperthermia*. *IEEE Trans. Microwave Theory Tech.*, **44**(10): 1755–1761, 1996.

[Dubois et al., 2000] L. Dubois, C. Vanoverschelde, V. Thomy, J. P. Sozanski and M. Chive. *Temperature control by microwave raiometry with narrow bandwidth*. *The European Physical Journal Applied Physics in Medicine and Biology*, **9**: 63–68, 2000.

[Edwards and Sinsky, 1992] M. Edwards and J. Sinsky. *A new criterion for linear 2-port stability using a single geometrically derived parameter*. *IEEE Transactions on Microwave Theory and Techniques*, **40**(12): 2303–2311, Dec 1992.

[Egan and Liu, 1995] G. F. Egan and Z.-Q. Liu. *Computers and networks in medical and healthcare systems*. *Comput. Biol. Med.*, **25(3)**: 355–365, 1995.

[Enander and Larson, 1974] B. Enander and G. Larson. *Microwave radiometric measurements of the temperature inside a body*. *Electronics Letters*, **10**: 317, 1974.

[Enz et al., 1987] C. Enz, E. Vittoz and F. Krummenacher. *A CMOS chopper amplifier*. *Solid-State Circuits, IEEE Journal of*, **22**(3): 335 – 342, jun 1987.

[Fear et al., 2002a] E. Fear, S. Hagness, P. Meaney, M. Okoniewski and M. Stuchly. *Enhancing breast tumor detection with near-field imaging*. *Microwave Magazine, IEEE*, **3**(1): 48 –56, March 2002a.

[Fear et al., 2002b] E. Fear, X. Li, S. Hagness and M. Stuchly. *Confocal microwave imaging for breast cancer detection: localization of tumors in three dimensions*. *Biomedical Engineering, IEEE Transactions on*, **49**(8): 812 –822, 2002b.

[Fear et al., 2002c] E. C. Fear, S. C. Hagness, P. M. Meaney, M. Okoniewski and M. A. Stuchly. *Enhancing breast tumor detection with near-field imaging*. *IEEE Microwave Magazine*, **3**(1): 48–56, March 2002c.

[Formica and Silvestri, 2004] D. Formica and S. Silvestri. *Biological effects of exposure to magnetic resonance imaging: an overview*. *BioMedical Engineering OnLine*, **3**(1): 11, 2004.

[Fujimoto, 1964] K. Fujimoto. *On the correlation radiometer technique*. *Microwave Theory and Techniques, IEEE Transactions on*, **12**(2): 203 – 212, mar 1964.

[Gabriel et al., 1996] S. Gabriel, R. W. Lau and C. Gabriel. *The dielectric properties of biological tissues: III. Parametric models for the dielectric spectrum of tissues*. *Physics in Medicine and Biology*, **41**(11): 2271–2293, 1996.

[Gong and Wang, 2009] Y. Gong and G. Wang. *Superficial tumor hyperthermia with flat left-handed metamaterial lens*. *Progress In Electromagnetics Research*, **98**: 389–405, 2009.

[Goodberlet and Mead, 2006] M. Goodberlet and J. Mead. *Two-load radiometer precision and accuracy*. *Geoscience and Remote Sensing, IEEE Transactions on*, **44**(1): 58 – 67, jan. 2006.

[Gotthardt et al., 2010] M. Gotthardt, C. P. Bleeker-Rovers, O. C. Boerman and W. J. Oyen. *Imaging of inflammation by pet, conventional scintigraphy, and other imaging techniques*. *Journal of Nuclear Medicine*, **51**(12): 1937–1949, 2010.

[Gunnarsson et al., 2008] S. Gunnarsson, A. Emrich, H. Zirath, R. Kozhuharov, C. Karnfelt, J. Embretsen and C. Tegnander. *A single-chip 53 GHz radiometer front-end MMIC for geostationary atmospheric measurements*. In *Radio and Wireless Symposium, 2008 IEEE*, pp. 867 –870. jan. 2008.

[Guyton and Hall, 2000] A. Guyton and J. Hall. *Textbook of Medical Physiology*. W.B. Saunders Company, The Curtis Center, Independence Squares West, Philadelphia, Pensylvania 19106, USA, tenth edition, 2000.

[Hagness et al., 1998] S. C. Hagness, A. Taflove and J. E. Bridges. *Two-Dimensinal FDTD Analysis of a Pulsed Microwave Confocal System for Breast Cancer Detection: Fixed-Focus and Antenna-Array Sensors*. *IEEE Trans. on Biomedical Eng.*, **45**(12): 1470–1479, December 1998.

[Haider and Chiao, 1999] B. Haider and R. Chiao. *Higher order nonlinear ultrasonic imaging*. In *Ultrasonics Symposium, 1999. Proceedings. 1999 IEEE*, volume 2, pp. 1527 –1531 vol.2. 1999.

[Hand et al., 2001] J. Hand, G. V. Leeuwen, S. Mizushina, J. V. de Kamer, K. Maruyama, T. Sugiura, D. Azzopardi and A. Edwards. *Monitoring of deep brain temperature in infants using multi-frequency microwave radiometry and thermal modelling*. *Phys. Med. Biol.*, **46**(7): 1885–1903, 2001.

[Harrer et al., 2003] J. U. Harrer, L. Mayfrank, M. Mull and C. Klötzsch. *Second harmonic imaging: a new ultrasound technique to assess human brain tumour perfusion*. *J Neurol Neurosurg Psychiatry*, **74**: 333–338, 2003.

[Head and Elliott, 2002] J. Head and R. Elliott. *Infrared imaging: making progress in fulfilling its medical promise*. *Engineering in Medicine and Biology Magazine, IEEE*, **21**(6): 80 –85, nov.-dec. 2002.

[Hendee and Ritenour, 2002] W. R. Hendee and E. R. Ritenour. *Medical Imaging Physics*. Wiley-Liss, Inc., fourth edition, 2002.

[Hurt, 1985] W. D. Hurt. *Multiterm debye dispersion relations for permittivity of muscle*. *Biomedical Engineering, IEEE Transactions on*, **BME-32**(1): 60 –64, jan. 1985.

[IFAC, 2011] IFAC. *An internet resource for the calculation of the dielectric properties of body tissues*. Italian National Research Council Institute for Applied Physics, September 2011.

[Iniewski, 2009] K. Iniewski. *Medical Imaging Principles, Detectors, and Electronics*. A John Wiley & Sons, Inc., Publication, 2009.

[Jacobsen and Birkelund, 2010] S. Jacobsen and Y. Birkelund. *Improved resolution and reduced clutter in ultra-wideband microwave imaging using cross-correlated back projection: Experimental and numerical results*. *International Journal of Biomedical Imaging*, **2010**: 1–10, 2010.

[Jacobsen and Klemetsen, 2008] S. Jacobsen and Ø. Klemetsen. *Improved detectability in medical microwave radio-thermometers as obtained by active antennas*. *IEEE Transactions on Biomedical Engineering*, **55**(12): 2778–2785, Dec. 2008.

[Jacobsen and Stauffer, 2001] S. Jacobsen and P. Stauffer. *Performance Evaluation of Various Antenna Configurations for Microwave Thermography During Superficial Hyperthermia*. *Journal Electrom. Waves App.*, **15**(1): 111–120, 2001.

[Jacobsen and Stauffer, 2002] S. Jacobsen and P. Stauffer. *Multifreqency Radiometric Determination of Temperature Profiles in a Lossy Homogeneous Phantom Using a Dual-Mode Antenna With Integral Water Bolus*. *IEEE Trans. Microwave Theory Tec.*, **50**(7): 1737–1746, 2002.

[Jacobsen et al., 2000] S. Jacobsen, P. Stauffer and D. Neuman. *Dual-Mode Antenna Design for Microwave Heating and Noninvasive Thermometry of Superficial Tissue Disease*. *IEEE Trans. Biomed. Eng.*, **47**(11): 1500–1509, 2000.

[Jacobsen et al., 2005] S. Jacobsen, H. Rolfsnes and P. Stauffer. *Characteristics of Microstrip Muscle-Loaded Single-Arm Archimedean Spiral Antennas as Investigated by FDTD Numerical Computations*. *IEEE Trans. Bio. Eng.*, **52**(2): 321–330, February 2005.

[Jemal et al., 2008] A. Jemal, R. Siegel, E. Ward, Y. Hao, J. Xu, T. Murray and M. J. Thun. *Cancer statistics, 2008*. *CA Cancer J Clin*, **58**(2): 71–96, 2008.

[Jovanov et al., 2005] E. Jovanov, A. Milenkovic, C. Otto and P. C. de Groen. *A wireless body area network of intelligent motion sensors for computer assisted physical rehabilitation*. *Journal of NeuroEngineering and Rehabilitation*, **2(6)**: pp 10, 2005.

[Kalender, 2006] W. A. Kalender. *X-ray computed tomography*. *Physics in Medicine and Biology*, **51**: R29–R43, 2006.

[Karanasiou et al., 2004a] I. Karanasiou, N. Uzunoglu and C. Papageorgiou. *Towards functional noninvasive imaging of excitable tissues inside the human body using focused microwave radiometry*. *Microwave Theory and Techniques, IEEE Transactions on*, **52**(8): 1898 – 1908, aug. 2004a.

[Karanasiou et al., 2004b] I. Karanasiou, N. Uzunoglu, S. Stergiopoulos and W. Wong. *A passive 3d imaging thermograph using microwave radiometry*. *ITBM-RBM*, **25**(4): 227 – 239, 2004b.

[Kennedy et al., 2009] D. A. Kennedy, T. Lee and D. Seely. *A comparative review of thermography as a breast cancer screening technique*. *Integrative Cancer Therapies*, **8**(1): 9–16, 2009.

[Klemetsen and Jacobsen, 2011] Ø. Klemetsen and S. Jacobsen. *Improved radiometric performance attained by an elliptical microwave antenna with suction*. *Biomedical Engineering, IEEE Transactions on*, **PP**(99): 1, 2011.

[Klemetsen et al., 2011] Ø. Klemetsen, Y. Birkelund, S. K. Jacobsen, P. F. Maccarini and P. R. Stauffer. *Design of medical radiometer front-end for improved performance*. *Progress In Electromagnetics Research B*, **27**: 289–306, 2011.

[Land, 1987] D. Land. *A clinical microwave thermography system*. *Physical Science, Measurement and Instrumentation, Management and Education - Reviews, IEE Proceedings A*, **134**(2): 193 –200, february 1987.

[Land, 2001] D. V. Land. *An efficient, accurate and robust radiometer configuration for mocrowave temperature measurement for industrial and medical applications*. *Journal of Microwave Power & Electromagnetic Energy*, **36**(3): 139–153, 2001.

[Land et al., 2007] D. V. Land, A. P. Levick and J. W. Hand. *The use of the Allan deviation for the measurement of the noise and drift performance of microwave radiometers*. *Measurement Science Technology*, **18**(7): 1917 –1928, 2007.

[Larsi et al., 1999] T. Larsi, K. Ridaoui, B. Bocquet, A. Mamouni and Y. Leroy. *Absolute Wighting Functions for Near-Field Microwave Radiometric Applications*. *Journal of Electromagnetic Waves and Applications*, **13**: 1237–1265, 1999.

[Lazebnik et al., 2006] M. Lazebnik, M. C. Converse, J. H. Booske and S. C. Hagness. *Ultrawideband temperature-dependent dielectric properties of animal liver tissue in the microwave frequency range*. *Phys. Med. Biol.*, **51**: 1941–1955, 2006.

[Leroy et al., 1987] Y. Leroy, A. Mamouni, J. V. D. Velde, B. Bocquet and B. Dujardin. *Microwave Radiometry For Non-invasive Thermometry*. *Automedica*, **8**: 181–202, 1987.

[Leroy et al., 1998] Y. Leroy, B. Bocquet and A. Mamouni. *Non-invasive microwavew radiometry thermometry*. *Physiol. Meas.*, **19**: 127–148, 1998.

[Luo et al., 2008] H. Luo, W. J. Sehnert, J. S. Ellinwood, D. Foos, B. Reiner and E. Siegel, eds. *Motion blur detection in radiographs*, volume Proc. SPIE 6914, 69140U (2008);. SPIE, February 2008.

[Mo et al., 2007] T. T. Mo, Q. Xue and C. H. Chan. *A broadband compact microstrip rat-race hybrid using a novel cpw inverter*. *IEEE Trans. Microw. Theory Tech.*, **55**(1): 161–167, January 2007.

[Norris, 2002] A. C. Norris. *Essentials of Telemedicine and Telecare*. John Wiley and Sons, 2002.

[Obstfelder et al., 2007] A. Obstfelder, K. Engeseth and R. Wynn. *Characteristics of successfully implemented telemedical applications*. *Implementation Science*, **2**(1): 25, 2007.

[Ohanian, 1985] H. Ohanian. *Physics*. W.W.Norton and Company, Inc, 500 Fifth Avenue, New York, first edition, 1985.

[Ohinmaa et al., 2001] A. Ohinmaa, D. Hailey and R. Roine. *Elements for assessment of telemedicine applications*. *International Journal of Technology Assessment in Health Care*, **17**(02): 190–202, 2001.

[Oikonomou et al., 2009] A. Oikonomou, I. S. Karanasiou and N. K. Uzunoglu. *Potential brain imaging using near field radiomety*. *Journal of Instrumentation*, **4**(05): P05017, 2009.

[Oikonomou et al., 2010] A. Oikonomou, I. S. Karanasiou and N. K. Uzunoglu. *Phased-array near field radiometry for brain intracranial applications*. *Progress In Electromagnetics Research*, **109**: 345–360, 2010.

[Ossberger et al., 2004] G. Ossberger, T. Buchegger, E. Schimback, A. Stelzer and R. Weigel. *Non-invasive respiratory movement detection and monitoring of hidden humans using ultra wideband pulse radar*. In *Ultra Wideband Systems, 2004. Joint with Conference on Ultrawideband Systems and Technologies. Joint UWBST IWUWBS. 2004 International Workshop on*, pp. 395 – 399. may 2004.

[Pavlopoulos and Delopoulos, 1999] S. Pavlopoulos and A. Delopoulos. *Designing and implementing the transition to a fully digital hospital*. *Information Technology in Biomedicine, IEEE Transactions on*, **3**(1): 6 –19, march 1999.

[Powell and Chandrakasan, 2004] J. Powell and A. Chandrakasan. *Differential and single ended elliptical antennas for 3.1-10.6 GHz ultra wideband communication*. p. 2935 2938. Proceedings of the IEEE Antennas and Propagation Society Symposium, Monterey, California, USA, June 2004.

[Pozar, 1998] D. Pozar. *Microwave Engineering*. Wiley, second edition, 1998.

[Pozar, 2004] D. M. Pozar. *Microwave Engineering*. John Wiley and Sons, third edition, 2004.

[Reeves et al., 1975] R. Reeves, A. Anson and D. Landen. *Manual of Remote Sensing*, volume I. American Society of Photogrammetry,Virginia,USA., 105 N, Virginia Ave. Falls Church, Va 22046, first edition, 1975.

[Rengarajan, 1989] S. Rengarajan. *Compound radiating slots in a broad wall of a rectangular waveguide. Antennas and Propagation, IEEE Transactions on*, **37**(9): 1116 –1123, sep 1989.

[Rietveld et al., 1999] P. J. M. Rietveld, W. L. J. Van-Putten, J. Van-Der-Zee and G. C. Van-Rhoon. *Comparison of the clinical effectiveness of the 433 MHz LUCITE CONE applicator with that of a conventional waveguide applicator in applications of superficial hyperthermia. Int. J. Radiation Oncology Bil. Phys.*, **43(3)**: 681–687, 1999.

[Riley, 2008] W. Riley. *Handbook of Frequency Stability Analysis*. U. S. Government printing office. Washington, 2008.

[Samaras et al., 2000] T. Samaras, P. Rietveld and G. Van-Rhoon. *Effectiveness of FDTD in predicting SAR distributions from the lucite cone applicator. Microwave Theory and Techniques, IEEE Transactions on*, **48**(11): 2059 – 2063, nov 2000.

[Schrope and Newhouse, 1993] B. A. Schrope and V. L. Newhouse. *Second harmonic ultrasonic blood perfusion measurement. Ultrasound in Med.and Biol.*, **19(7)**: 567–579, 1993.

[Semelka et al., 2007] R. C. Semelka, D. M. Armao, J. Elias and W. Huda. *Imaging strategies to reduce the risk of radiation in ct studies, including selective substitution with mri. Journal of Magnetic Resonance Imaging*, **25**(5): 900–909, 2007.

[Sha et al., 2002] L. Sha, E. Ward and B. Stroy. *A review of dielectric properties of normal and malignant breast tissue*. In *SoutheastCon, 2002. Proceedings IEEE*, pp. 457 –462. 2002.

[Sharkov, 2003] E. A. Sharkov. *Passive Microwave Remote Sensing of the Earth*. Praxis Publishing, 2003.

[Skou and Vine, 2006] N. Skou and D. L. Vine. *Microwave Radiometer Systems Design and Analysis*. Artech House, second edition, 2006.

[Smith et al., 2010] Z. A. Smith, N. Postma and D. Wood. *Fast scanning in the developing world emergency department. S Afr Med J.*, **100(2)**: 105–108, 2010.

[Snow et al., 2011a] B. Snow, K. Arunachalam, V. De-Luca, P. Maccarini, Ø. Klemetsen, Y. Birkelund, T. Pysher and P. Stauffer. *Non-invasive vesicoureteral reflux detection: Heating risk studies for a new device. Journal of Pediatric Urology*, **In Press, Corrected Proof**: –, 2011a.

[Snow, 2011] B. W. Snow. *New noninvasive methods to diagnose vesicoureteral reflux. Pediatric Urology. Current Opinion in Urology*, **21(4)**: 339 – 342, 2011.

[Snow and Taylor, 2010] B. W. Snow and M. B. Taylor. *Non-invasive vesicoureteral reflux imaging. Journal of Pediatric Urology*, **6 issue 6**: 543 – 549, 2010.

[Snow et al., 2011b] B. W. Snow, K. Arunachalam, V. De-Luca, Ø. Klemetsen, Y. Birkelund, P. Stauffer and P. Maccarini. *Noninvasive grade v vesicoureteral reflux detection: An animal study*. *The Internet Journal of Urology*, **185**: e232–e232, 2011b.

[Sprawls, 1987] P. Sprawls. *Physical Principles of Medical Imaging*. Lippincott Williams and Wilkins, 1987.

[Staderini, 2002] E. Staderini. *Uwb radars in medicine*. *Aerospace and Electronic Systems Magazine, IEEE*, **17**(1): 13 –18, jan 2002.

[Stauffer and Maccarini, 2011] P. Stauffer and P. Maccarini. *Evolution of antenna performance for applications in thermal medicine*. In *Antennas and Propagation (EUCAP), Proceedings of the 5th European Conference on*, pp. 3080 –3083. april 2011.

[Stauffer et al., 1998] P. Stauffer, F. Rossetto, M. Leencini and G. Gentilli. *Radiation patterns of dual concentric conductor microstrip antennas for superficial hyperthermia*. *IEEE Transactions on Biomedical Engineering*, **45**(5): 605 –613, may. 1998.

[Stauffer et al., 2010] P. R. Stauffer, P. Maccarini, K. Arunachalam, O. Craciunescu, C. Diedrich, T. Juang, F. Rossetto, J. Schlorff, A. Milligan, J. Hsu, P. Sneed and Z. Vujaskovic. *Conformal microwave array (CMA) applicators for hyperthermia of diffuse chest wall recurrence*. *Int. J. Hyperthermia*, **26(7)**: 686 698, 2010.

[Stauffer et al., 2011] P. R. Stauffer, P. F. Maccarini, V. De-Luca, S. Salahi, A. Boico, K. Arunachalam, Ø. Klemetsen, Y. Birkelund, S. K. Jacobsen, F. Bardati, P. Tognolotti and B. Snow. *Microwave radiometry for non-invasive detection of vesicoureteral reflux (VUR) following bladder warming*. Society of Photo-Optical Instrumentation Engineers (SPIE), January 22-27 2011.

[Stec and Susek, 2000] B. Stec and W. Susek. *A 4.4 GHz microwave thermometer with compensation of reflection coefficient*. *13th Int. Conf. Micro., Radar Wirel. Commun. Wroclaw, Poland*, pp. 453–456, 2000.

[Stec et al., 2004] B. Stec, A. Dobrowolski and W. Susek. *Multifrequency microwave thermograph for biomedical applications*. *Journal of telecommunications and Information Technology*, (1): 117–122, 2004.

[Stout and Zaidi, 2008] D. B. Stout and H. Zaidi. *Preclinical multimodality imaging in vivo*. *PET Clinics*, **3**(3): 251 – 273, 2008. PET/CT and PET/MRI for Assessment of Structural and Functional Relationships in Disease Conditions.

[Sugiura et al., 2004] T. Sugiura, Y. Kouno, A. Hashizume, H. Hirata, J. Hand, Y. Okita and S. Mizushina, eds. *Five-band microwave radiometer system for non-invasive measurement of brain temperature in new-born infants: system calibration and its feasibility*. Proceedings of the 26th Annual Internatinal Conference of the IEEE EMBS. San Francisco, CA, USA, September 1-5, 2004.

[Tiuri, 1964] M. E. Tiuri. *Radio astronomy receivers. IEEE Trans. Antennas Propagat.*, **12**: 930 938, 1964.

[Townsend et al., 2004] D. W. Townsend, J. P. J. Carney, J. T. Yap and N. C. Hall. *PET/CT Today and Tomorrow. The Journal of Nuclear Medicine*, **45(1) Suppl**: 4S–14S, 2004.

[Ulaby et al., 1981] F. Ulaby, R. Moore and A. Fung. *Microwave Remote Sensing*, volume I Microwave Remote Sensing Fundamentals and Radiometry. Artec House, 685 Canton Street, Norwood, MA 02062, USA, first edition, 1981.

[Ulaby et al., 1986] F. T. Ulaby, R. K. Moore and A. K. Fung. *Microwave Remote Sensing Active and Passive*, volume III From Theory to Applications. Artech House, 685 Canton Street, Norwood, MA 02062, USA, reprint 1990 edition, 1986.

[Van-Rhoon et al., 1998] G. C. Van-Rhoon, P. J. M. Rietveld and J. Van-Der-Zee. *A 433 MHz Lucite Cone waveguide applicator for superficial hyperthermia. Int. J. Hyperthermia*, **14(1)**: 13–27, 1998.

[Varray et al., 2011] F. Varray, A. Ramalli, C. Cachard, P. Tortoli and O. Basset. *Fundamental and second-harmonic ultrasound field computation of inhomogeneous nonlinear medium with a generalized angular spectrum method. Ultrasonics, Ferroelectrics and Frequency Control, IEEE Transactions on*, **58**(7): 1366 –1376, july 2011.

[Vesnin, 2011] S. Vesnin. *Thermal Imaging System*. http://www.resltd.ru/eng/rtm/training.php, September 2011.

[Wang and Leedham, 2006] L. Wang and G. Leedham. *Near- and far- infrared imaging for vein pattern biometrics. Advanced Video and Signal Based Surveillance, IEEE Conference on*, pp. 52–52, Nov 2006.

[Woods, 1976] D. Woods. *Reappraisal of the unconditional stability criteria for active 2-port networks in terms of s parameters. Circuits and Systems, IEEE Transactions on*, **23**(2): 73 – 81, feb 1976.

[Wyatt, 2010] C. R. Wyatt. *Development of MR Thermometry Strategies for Hyperthermia of Extremity and Breast Tumors*. Ph.D. thesis, Department of Biomedical Engineering in the Graduate School of Duke University, 2010.

[Xie et al., 2006] Y. Xie, B. Guo, L. Xu, J. Li and P. Stoica. *Multistatic adaptive microwave imaging for early breast cancer detection. Biomedical Engineering, IEEE Transactions on*, **53**(8): 1647 –1657, aug. 2006.

[Zharov et al., 2004] V. P. Zharov, S. Ferguson, J. F. Eidt, P. C. Howard, L. M. Fink and M. Waner. *Infrared imaging of subcutaneous veins. Lasers in Surgery and Medicine*, **34**(1): 56–61, 2004.

[Zhurbenko, 2011] V. Zhurbenko. *Challenges in the design of microwave imaging systems for breast cancer detection*. *Advances in Electrical and Computer Engineering*, **11(1)**: pp 6, 2011.

[Zito et al., 2007] D. Zito, D. Pepe, B. Neri, D. De Rossi, A. Lanata, A. Tognetti and E. Scilingo. *Wearable system-on-a-chip uwb radar for health care and its application to the safety improvement of emergency operators*. In *Engineering in Medicine and Biology Society, 2007. EMBS 2007. 29th Annual International Conference of the IEEE*, pp. 2651 –2654. aug. 2007.

[Zwally, 1977] H. J. Zwally. *Microwave emissivity and accumulation rate of polar firn*. *Journal of Glaciology*, **18(79)**: pp 21, 1977.

Chapter 6

Papers:

6.1 Published Paper: Design of Medical Radiometer Front-end for Improved Performance

6.2 Paper in Review: Radiometric temperature reading of a hot ellipsoidal object inside the oral cavity by a shielded microwave antenna put flush to the cheek

6.3 Accepted Paper, IEEE Early Access: Improved Radiometric Performance Attained by an Elliptical Microwave Antenna With Suction

6.4 Published Paper: Vesicoureteral Reflux in Children: A phantom Study of Microwave Heating and Radiometric Thermometry of P ediatric Bladder

6.5 Published Paper: Improved Detectability in Medical Microwave Radio-Thermometers as Obtained by Active Antennas

ISBN xxx-xx-xxxx-xxx-x